Renewable Energy 218 (2023) 119331

Contents lists available at ScienceDirect

Renewable Energy

journal homepage: www.elsevier.com/locate/renene

Revisiting salt hydrate selection for domestic heat storage applications

Natalia Mazur [a,b,e], Melian A.R. Blijlevens [c], Rick Ruliaman [a,d], Hartmut Fischer [e], Pim Donkers [f], Hugo Meekes [c], Elias Vlieg [c], Olaf Adan [a,b,e,f], Henk Huinink [a,b,*]

[a] Technical University Eindhoven, P.O. Box 513, Department of Applied Physics, 5600, MB, Eindhoven, the Netherlands
[b] Eindhoven Institute for Renewable Energy Systems, Eindhoven University of Technology, PO Box 513, 5600 MB, Eindhoven, the Netherlands
[c] Radboud University, Institute for Molecules and Materials, Heyendaalseweg 135, 6525, ED, Nijmegen, the Netherlands
[d] ICL Specialty Fertilizers, Nijverheidsweg 1-5, 6422 PD, Heerlen, the Netherlands
[e] The Netherlands Organization for Applied Scientific Research (TNO), High Tech Campus 25, 5656, AE, Eindhoven, the Netherlands
[f] Cellcius, Horsten 1, 5612 AX, Eindhoven, the Netherlands

ARTICLE INFO

Keywords:
Salt hydrates
Thermochemical heat storage
Database
Material selection

ABSTRACT

In this work, we evaluate 454 salt hydrates and 1073 unique hydration reactions in search of suitable materials for domestic heat storage. The salts and reactions are evaluated based on their scarcity, toxicity, (chemical) stability and energy density (>1 GJ/m^3) and alignment with 3 use case scenarios. These scenarios are based on space heating (T > 30 °C) and hot water (T > 55 °C) to be provided by discharge as well as on heat sources available in the built environment (T < 160 °C) for charging. From all evaluated materials, only 8 salts and 9 reactions (K_2CO_3 0–1.5, LiCl 0–1, NaI 0–2, $NaCH_3COO$ 0–3, $(NH_4)_2Zn(SO_4)_2$ 0–6, $SrBr_2$ 1–6, CaC_2O_4 0–1, $SrCl_2$ 0–1 and 0–2) fulfil all of the criteria. Provided a suitable stabilisation method is found additional 4 salts and 13 reactions ($CaBr_2$ 6-0, $CaCl_2$ 6-0, 6-1, 6-2, 4-0, 4-1, 4-2, LiBr 2-0, 2-1, 2-0, LiCl 2-0, 2-1, $ZnBr_2$ 2-0) From this selection, only 2 salts/reactions (NaI and $(NH_4)_2Zn(SO_4)_2$) have not been extensively studied in the literature. Moreover, many well-investigated salt hydrates, such as $MgSO_4$ and LiOH, did not pass our screening. This work underlines the scarcity of materials suitable for domestic applications and the need to broaden the scope of future evaluations.

1. Introduction

With the ongoing energy transition, the integration of renewable energy sources into the energy landscape has been steadily increasing [1]. A greater impact of that progress is expected if the mismatch in space and time between renewable energy generation and utilization [2] is overcome through an energy storage solution. The required energy storage depends on the final application, as energy is produced and used in various forms. The residential sector consumes 21% of the total energy [3]. Nearly 80% of that is consumed as thermal energy for space heating and hot tap water [4]. Therefore, a significant contribution to energy transition could be made by tackling thermal energy demand through heat storage on a domestic level.

Domestic heat storage can be realised in three forms: sensible, latent and thermochemical heat storage (TCHS). Further, each heat storage solution can be subdivided into several categories based on the materials used to store heat and their working principle [5]. The basis for TCHS is often a reversible gas-solid reaction, where water, ammonia or methanol vapour is the used gas. However, for safety and environmental reasons, reactions utilising H_2O are most common for domestic applications [6]. The materials used for TCHS are called thermochemical materials (TCM). The great advantage of this solution over other heat storage systems is the possibility of long-term, nearly loss-free energy storage. Because TCHS is based on a reaction between two components, the energy is released only when both reactants are in contact with each other. Sensible and latent heat storage are based on only the temperature change of the storage material. Therefore, they are prone to self-discharge due to heat dissipation.

In the past decade, TCHS, based on a chemical reaction between a salt hydrate and water vapour (see Fig. 1 and Reaction 1), has gradually gained more interest [7]. Next to the loss-free, long-term energy storage, relatively high energy density, and low temperature operating window suitable for built environment have drawn researchers towards this category of materials.

$$Salt \cdot mH_2O(s) + (n-m)H_2O(g) \leftrightarrow Salt{\cdot}nH_2O(s) + Q \quad \text{(Rx.1)}$$

* Corresponding author. Technical University Eindhoven, P.O. Box 513, Department of Applied Physics, 5600, MB, Eindhoven, the Netherlands.
E-mail address: h.p.huinink@tue.nl (H. Huinink).

https://doi.org/10.1016/j.renene.2023.119331
Received 7 June 2023; Received in revised form 21 August 2023; Accepted 15 September 2023
Available online 15 September 2023

In the initial state, salt has *m* moles of water per mole of salt where m $\geq$ 0. During the reaction, the salt reversibly reacts with water vapour, $H_2O(g)$, and incorporates water molecules into its crystal structure. The reaction releases heat, *Q*. After the reaction, the salt has *n* moles of water per mole of salt where n > m. The water incorporated into the salt's crystal structure is referred to as water of crystallisation or crystal water. The water uptake can happen in one or several steps depending on the salt. Each step corresponds to a well-defined hydration state before salt reaches its maximum loading. After reaching maximum hydration, exposure to high water vapour pressure may lead to deliquescence, i.e. formation of salt solution, sometimes referred to as overhydration.

The thermochemical reaction described above is the foundation of TCHS based on salt hydrates. The heat is stored by removing crystal water from the salt's structure, thus charging the system. An external heat source has to be used since this process is endothermic. The dehydration reaction (right to left in Fig. 1) corresponds to charging. The stored heat is released during discharge when water vapour from an external water reservoir is reintroduced to the system, and the salt is hydrated. As mentioned above, water (re)incorporation into the crystal structure is exothermic. Thus, the generated heat is harvested by, for example, heat exchangers. Therefore the hydration reaction (left to right in Fig. 1) is the discharge reaction. The reversible formation and breakage of chemical bonds between the two reactants and the energy involved in that reaction enable heat storage. However, the material's intrinsic properties, such as, for example, crystal structure and elemental composition, determine the reaction rate and the conditions at which the system is (dis)charged. Therefore, these properties are critical for the final power output of the system and its suitability for practical application.

For an entire domestic TCHS system (see example in Fig. 2), the operating conditions, i.e. charge and discharge conditions, are primarily determined by the water vapour and heat source. Here we consider a typical case of charging and discharging conditions reliant on water and heat sources, although other configurations are possible. An underground water reservoir can be used to generate the required water vapour during the discharge cycle and condense the vapour generated during the charge cycle. The necessary heat for charging comes from solar thermal collectors installed on the house's roof. The operating temperature of those two components, together with the temperature demand of space heating and hot tap water, determines the system's boundary conditions, i.e. maximum dehydration temperature and minimum hydration temperature.

The primary benefit of a TCHS system is its ability to store energy for a long time, nearly loss-free. It is achievable because of the nature of the reactants (gas and solid), making it easy to be fully separated during the storage period, preventing self-discharge. The only energy losses occur during system operation due to sensible heat losses when parts of the system heat up due to hydration. Further, salt hydrates have a higher energy density than other heat storage systems and other thermochemical materials (TCMs) considered for similar end-use [8]. Finally, many salts are eco-friendly, non-toxic and readily available in bulk or even as a byproduct of industrial processes, making them affordable. It has been estimated that material costs can make up approximately 30% of the total system cost [9], which amplifies the importance of correct TCM choice.

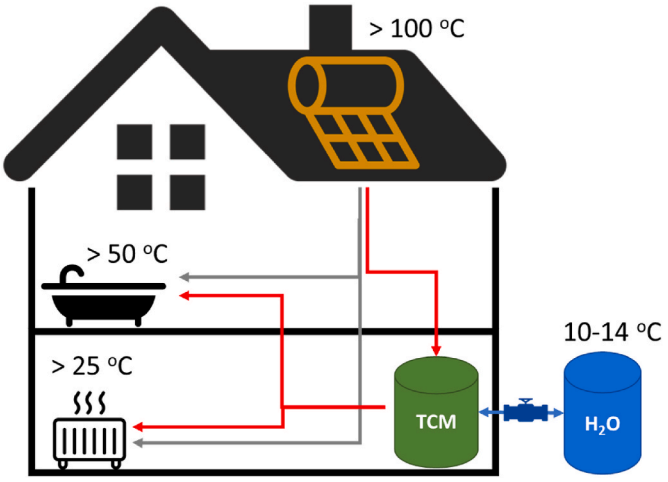

Fig. 2. Sketch of a domestic TCHS with solar thermal collectors on the roof (yellow), a heat storage unit (green) and a coupled water reservoir (blue). Arrows show heat supply paths directly from solar collectors (grey) or via the heat storage unit (red).

Since the early 2000s, many reviews have been published evaluating materials and attempting to choose the most suitable one for a predefined application [9–22]. The potential candidates were usually identified based on a literature study or numerical analysis and evaluated based on theoretical energy density and theoretical equilibrium phase transition temperature, T_{eq}, described by thermodynamics. The theoretical energy density is based on reaction enthalpy and material density. It is often compared with other heat storage principles [12] or estimates of energy usage in a single-family home [9,18]. Those considerations result in a target energy density of the salt of 2 GJ/m^3, which is at the higher end of the energy density spectrum for potential TCM candidates [15,18,19].

The equilibrium phase transition temperature defines both hydration and dehydration temperature. In Fig. 1, heat generated during discharge or supplied during charge occurs at this temperature. There are two primary considerations for T_{eq}: 1) How it is calculated, and 2) What is the acceptable temperature range. The end application determines the latter, with the suggested discharge temperatures varying between 50 and 60 °C and charge temperatures varying between 130 and 155 °C. This selection is guided by the temperature requirements for domestic hot water (DHW) and the available heat source. Only one work by Essen et al. [13] considers a lower hydration temperature of 40 °C sufficient for domestic space heating (DSH). Donkers et al. [18] have shown that many reactions have T_{eq} between 30 and 50 °C. It means that the desire to satisfy DHW demand, which is only 19% of the overall thermal energy consumption [4], pre-emptively rejects many salts that could provide space heating.

The aim of this study is to re-evaluate data gathered on salt hydrate-water vapour reactions and assess their suitability as a domestic TCM under several use case scenarios that reflect different operating

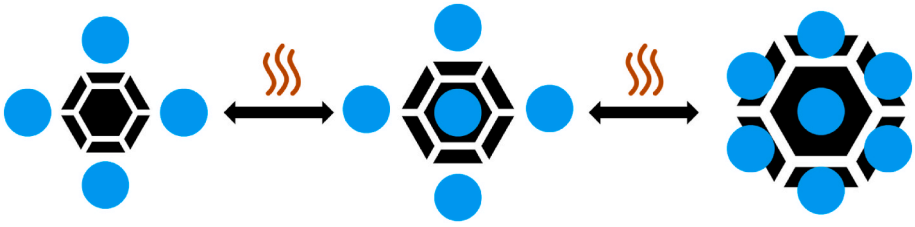

Fig. 1. A principle of hydration-dehydration reaction between salt hydrate (black crystal) and water (blue circle). Q (orange) is the heat released/supplied during the reaction, the image shows two consecutive hydration reactions.

conditions, including TCHS for domestic space heating only and TCHS combined with an external high temperature source. The starting point for this evaluation is the database compiled by Donkers et al. [18], which was expanded during our study. Furthermore, this evaluation is supplemented with experimental verification of some select candidates. We thus generate a list of potential TCM materials applicable to various use case scenarios that can be used for future studies.

2. Quantitative parameters

2.1. Reaction temperatures

The thermodynamic phase transition line between two hydration states of salt is described by the following relation between the water vapour pressure and the equilibrium temperature [18]:

$$\frac{p_{vap}}{p_0} = \exp\left(\frac{\Delta S^0}{R} - \frac{\Delta H^0}{RT_{eq}}\right) \quad (1)$$

where p_{vap} (mbar) is water vapour pressure, and p_0 (mbar) is reference vapour pressure set as the atmospheric pressure of 1000 mbar. Further, ΔS^0 (J/K mol H_2O) and ΔH^0 (kJ/mol H_2O) are entropy and enthalpy of the dehydration reaction per mol H_2O given in Reaction 1, R is the gas constant, and T_{eq} (K) is the corresponding transition temperature.

ΔH^0 *and* ΔS^0 are calculated from tabulated values for formation enthalpy $\Delta_f H^0$ (kJ/mol) and entropy $\Delta_f S^0$*(J/mol K)* of individual compounds partaking in the reaction, defined in the dehydration direction, an example of which is shown in Equation (2).

$$\Delta H^0 = \frac{\Sigma\Delta_f H^0_{products} - \Sigma\Delta_f H^0_{reactants}}{(n-m)} \quad (2)$$

where (*n-m*) is the number of moles of water partaking in the reaction.

By solving Equation (1) for a range of T and p_{vap} values, equilibrium conditions between two hydration states are obtained and commonly expressed as T_{eq} for a given p_{vap}. In Fig. 3, those equilibrium conditions are indicated by the thick solid black lines which separate the grey zones, which are the thermodynamically stable regions for individual hydration states.

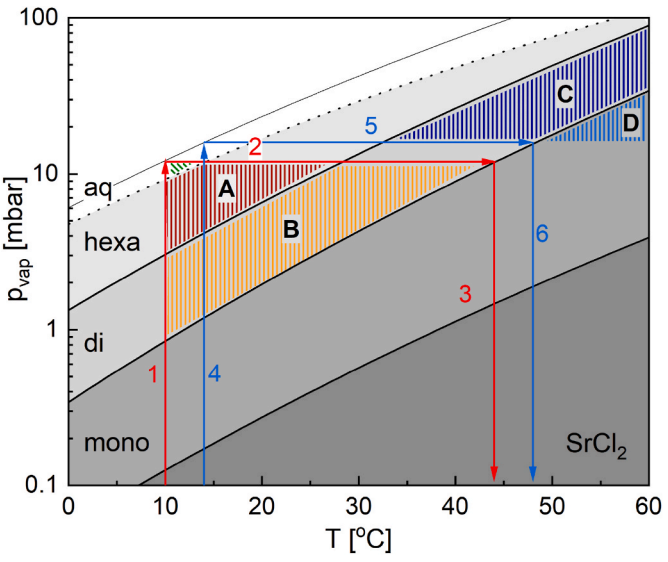

Fig. 3. A pressure-temperature phase diagram of $SrCl_2$ based on [23,24]. The grey zones mark distinct, stable hydration states. The dotted line indicates salt deliquescence, while pure water saturation pressure, calculated following the Antoine equation, is marked with the thin line. Orange lines (B) mark the zone where at 12 mbar $SrCl_2{\cdot}H_2O$ will hydrate to $SrCl_2{\cdot}2H_2O$, while the red lines (A) mark conditions where $SrCl_2{\cdot}2H_2O$ will hydrate to $SrCl_2{\cdot}6H_2O$ at 12 mbar. The navy lines (C) mark where $SrCl_2{\cdot}6H_2O$ will dehydrate to $SrCl_2{\cdot}2H_2O$ if water vapour is condensed at 16 mbar, and the blue area (D) is where $SrCl_2{\cdot}2H_2O$ dehydrates to $SrCl_2{\cdot}H_2O$. The green lines mark the zone where $SrCl_2{\cdot}6H_2O$ goes into deliquescence at 12 mbar.

In this example, p-T stability regimes of four hydration states, 0, 1-, 2- and 6-hydrate, of $SrCl_2$ are visualised. Based on those data, we can evaluate the suitability of $SrCl_2$ as TCM. As boundary conditions, we assume a water source at 10 °C, which gives a partial pressure of 12 mbar (red arrow 1). If we consider a hydration reaction of mono-to dihydrate, we see that the maximum attainable hydration temperature is approximately 45 °C (red arrows 2–3). The orange lines (B) indicate the temperature range in which monohydrate will hydrate, provided a p_{vap} of 12 mbar. For dehydration of dihydrate (blue lines, D), we assume that the generated water vapour will condense at 14 °C (16 mbar, blue arrow 4). It means that heat of at least 49 °C has to be supplied to drive the water of crystallisation out of the salt (blue arrows 5–6).

Nevertheless, at 12 mbar, two other reactions can occur if the temperature changes. Firstly, if the temperature drops below 26 °C, dihydrate will hydrate and form 6-hydrate (red lines, A). Secondly, if the temperature drops below 15 °C, the hexahydrate will deliquescence (green region). Salt deliquescence is a first-order phase transition from solid to liquid at conditions characteristic of the salt [25]. It is a process in which salt absorbs more water than it can incorporate into its crystal structure and dissolves. The salt will recrystallise (effloresce) when surrounding conditions are changed such that one of the hydration states is stable in its solid form.

We can determine which phase transitions will occur by traversing the phase diagram at selected vapour pressure and temperature conditions. However, those are purely theoretical considerations. Many salt hydrates suffer from reaction hysteresis [20,26], meaning the actual reaction conditions deviate from the calculated equilibrium conditions. This discrepancy varies between salts, and it is difficult to predict from tabulated values. Salt hydrate solubility has been proposed as an indicator for the anticipated reaction hysteresis [27], but this was never verified. Previous works treat the relationship between p_{vap} and T_{eq} in two distinct ways. The numerical works [15,19] and the study by Visscher [16] assume that the water vapour pressure equals the ambient pressure of 1 bar. According to the Antoine equation, 1 bar of water vapour pressure is generated at a water temperature of 100 °C. In the case of domestic application, it is safe to assume that the water reservoir would have a much lower temperature, given that the output temperature does not have to exceed 60 °C. Other studies assumed it to be between 10 °C [18,28] and 20 °C [9], with corresponding p_{vap} values ranging from 10 to 23 mbar. Since high p_{vap} usually couples with high T_{eq}, the assumption of very high p_{vap} will lead to overestimating temperature output during hydration or material rejection due to excessively high dehydration temperature. Therefore, it is crucial that even theoretical material evaluation is done with practical conditions in mind.

2.2. Energy density

The amount of energy a salt hydrate can store is based on the reaction enthalpy ΔH^0 of a reaction shown in the reaction in Fig. 1. Further, the theoretical energy density corresponding to dehydration from hydration state n to m on the material level can be expressed on a gravimetric or volumetric basis.

The theoretical gravimetric energy density, ϵ_G, is defined as:

$$\epsilon_G = \frac{\Delta H^0 \cdot (n-m)}{M_n} \quad (3)$$

where M_n (kg/mol) is the molar mass of the highest hydrate partaking in the considered reaction.

The corresponding theoretical volumetric energy density, ϵ_V, is defined as:

$$\epsilon_V = \frac{\Delta H^0 \cdot (n-m)}{M_n} \rho_n = \epsilon_G \rho_n \quad (4)$$

where ρ_n (kg/m^3) is the crystal density of the highest hydrate partaking in the considered reaction. For a process where k hydration steps are considered, the theoretical volumetric energy density is calculated as:

$$\epsilon_V = \frac{\sum_{i=1}^{i=k} \Delta H^0 \cdot (n_i - m_i)}{M_n} \rho_n \quad (5)$$

2.3. Volumetric changes

During hydration and dehydration, the salt hydrate undergoes volume changes linked with water molecules entering or leaving the crystal structure. A first approximation of the extent of those changes, υ, can be made based on the crystal structure density. The expansion during hydration in volume percent υ is expressed as:

$$\upsilon = \left(1 - \frac{M_m}{\rho_m}\frac{\rho_n}{Mn}\right) \cdot 100\% \quad (6)$$

where M_m (kg/mol) and ρ_m (kg/m^3) are the molar mass and crystal mass density of the lowest hydrate partaking in the reaction. Large volumetric changes during cycling can cause issues with the mechanical stability of the material and lead to pulverisation and agglomeration of the storage unit [29,30].

2.4. Water footprint

The water vapour used for hydration or produced in dehydration has to be supplied or removed from the system, creating a need for a water reservoir and a system that will transport that water vapour. Depending on a system design, the water reservoir can be an intrinsic part of the system, and all of it is stored locally (closed system). Optionally, the water reservoir is placed outside TCHS and coupled with the unit only when needed (open system). Regardless of the system design, water vapour transport will occur during TCHS operation. The amount of water needed to release a certain amount of energy depends on reaction enthalpy, i.e. how much heat is released when a water molecule is incorporated into the crystal structure. Based on this, we can calculate the water footprint, V_{H2O}, for 1 GJ of energy according to:

$$V_{H2O} = \frac{10^6}{\Delta H^0 \cdot M_{H2O}} \quad (7)$$

where M_{H2O} (55.56 mol/L) is the molarity of pure water.

3. Selection procedure

The database initially generated by Donkers et al. [18] with 563 entries and based primarily on [31,32] has been expanded with new data mainly from Refs. [11,20,33] and other publications and currently encompasses over 2286 entries. Among those entries, there are 1074 unique reactions and 454 unique salts. All those entries have been subjected to a screening process sketched in Fig. 4. First, entries gathered in the database were screened according to the following screening filters: (1) elemental properties, (2) use case scenario, (3) energy density and (4) chemical and physical stability. If a material passed all the abovementioned screening filters, it was added to a long list. Next, we conducted a literature survey to identify potential hazards and other issues not identified by the initial filters. Again, materials that passed the literature study were put on the shortlist. Finally, we probed the reaction properties under experimental conditions, such as reversibility, kinetics and hysteresis. Salts and reactions that passed all those screening steps are the most promising candidates based on current selection criteria.

3.1. Elemental filter

The elemental filter criterion removes candidates encompassing the most obvious elements unsuitable in large quantities for the domestic environment. It covers elements classified as radioactive (Atomic numbers 84–118), toxic (heavy) metals (Be, Cr, Ba, As, Cd, Pb, Hg, Ni, Sb, Tl, Se, Co, Mn) [34–36], rare earth and precious metals (Ga, Ge, Ru, Rh, Pd, Ag, In, Te, Re, Os, Ir, Pt, Au, Bi, Sc, Y, atomic numbers 57–71) [37,38]. Salts containing elements in the first two classes are excluded because of health risks. Although some elements, such as Mn or Se, are necessary micronutrients, they become highly toxic in large quantities. The second two classes of elements are excluded due to their price, scarcity and already high demand in the industry. Nevertheless, those criteria can be subject to changes [39] if, for example, a particular salt is oversupplied [40].

3.2. Use case scenario filter

Next, we introduced a series of boundary conditions for charge and discharge requirements that determine potential use case scenarios. Based on that, we have calculated T_{eq} - p_{vap} relationships according to the method shown in Section 2 and assessed those values in relation to the predefined use case scenarios outlined below. Reactions that did not fulfil the desired charge and/or discharge temperatures were excluded from further evaluation.

We define our water reservoir conditions based on the average Western European climate. For example, a 7 m deep borehole will have

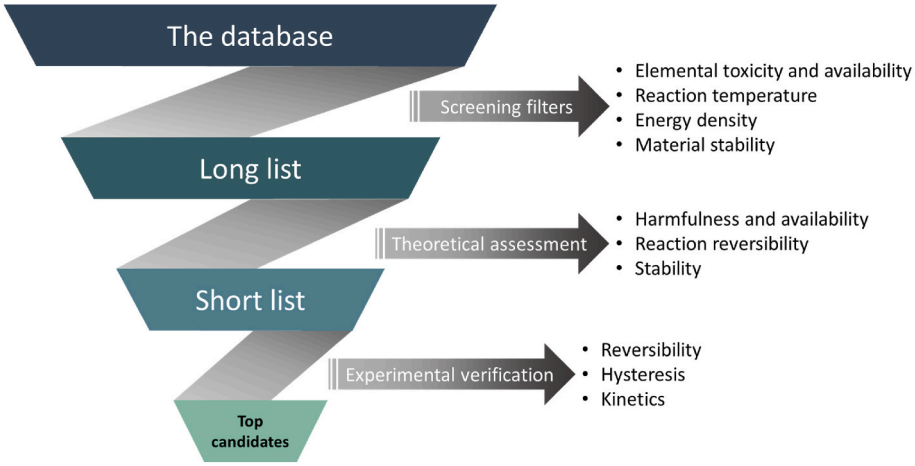

Fig. 4. Diagram showing different stages in the salt selection process and the causes for exclusion.

an approximate temperature of 12 °C [18,41,42]. Allowing for some temperature variations connected to a location, season and TCHS system operation, we assume two different water reservoir temperatures. For hydration or discharge, we adopt a water temperature of 10 °C resulting in a vapour pressure of 12 mbar. Optionally, the water temperature could be increased to 25 °C (31 mbar) by preheating it with an electrical heater or designing a cascade heat storage [43]. If an electric heater is used, the energy used to operate it must be considered when evaluating the overall energy density of TCHS and system cost. On the other hand, a cascade TCHS uses two or more salt hydrates in tandem, where the heat output of one of the salts is used as an input for the second one. In this case, both materials have to be considered when calculating material cost and the overall energy density. For dehydration or charge, we presuppose that the generated water vapour will condense at 14 °C or 16 mbar.

The available heat source also dictates the charge conditions. If we assume the use of solar thermal collectors, the expected maximum operating temperature output varies between 80 °C and 210 °C [44]. As maximum performance cannot be expected at all times while heat losses are, and the cost of high-temperature solar collectors is very high, we have chosen a temperature of 160 °C as the maximum dehydration temperature. It is a more realistic case but still pushes domestic solar collector capabilities [45]. Ideally, the salt hydrate should dehydrate below 100 °C as those temperatures are much more achievable for most solar thermal collectors, even during less sunny periods [46]. Moreover, other heat sources could be considered in the same temperature range, for example, electrical heaters powered by photovoltaic solar panels or heat pumps.

The heat generated during the hydration must fulfil the needs of space heating and/or hot tap water. Input temperature for space heating depends on the heating system installed in the house. Modern floor heating requires the lowest input temperature, while the international standards ISO 7730 and DIN EN 15251 state that 20–25 °C is a sufficient room temperature. Further, assuming a 5 K temperature loss due to sensible heat losses [47], a hydration temperature of 30 °C is sufficient to cover this demand.

In the case of hot tap water, input temperature is associated with the survival and growth of legionella bacteria, which thrives between 20 and 45 °C [48]. Depending on the country's legislation, the minimum DHW temperature has to be between 50 and 60 °C [49,50]. Thus, the hydration reaction should yield a minimum temperature of 55 °C to allow for sensible heat losses.

Based on the discussed requirements, we have identified three use case scenarios summarised in Fig. 5 and Table 1. Scenario 1 aims at providing at least DSH since, in many countries, space heating accounts for more than 60% of the total energy consumption [51], making it a prime contender for energy savings. Optionally, the low-temperature heat generated by the salt could be used as an input for a heat pump to increase its performance and still provide domestic hot water. Scenario 2 aims at providing both DSH and DHW. It also allows more flexibility in the space heating design, given that it provides higher output temperatures. Scenario 3 also aims to cover all domestic heating needs using a water source at elevated temperatures. However, it is the least cost-effective scenario, given that an additional heat source, such as a heat pump, must be incorporated into the system.

Table 1
Summary of boundary conditions, output hydration T, input dehydration T at a given p_{vap}, describing each use case scenario.

	Scenario 1	Scenario 2	Scenario 3
Minimum hydration conditions (discharge)	30 °C, 12 mbar	55 °C, 12 mbar	55 °C, 31 mbar
Maximum dehydration conditions (charge)	160 °C, 16 mbar	160 °C, 16 mbar	160 °C, 16 mbar

The vapour pressures, summarised in Table 1, together with enthalpy and entropy values gathered in the database, were used as input values for the thermodynamic calculations. We have compared the calculated T_{eq} with the temperatures in Table 1, which we have used as boundary conditions during the evaluation.

In the case of a multi-step process, first, we calculated T_{eq} for each transition before evaluating the entire process. The T_{eq} for the transition between the two highest-considered hydrates was taken as the maximum hydration temperature, while T_{eq} for the transition between the two lowest-considered hydrates was taken as the minimum dehydration temperature.

For example, we know that $SrCl_2$ has four hydration states. From Fig. 3, we obtain for scenarios 1 and 2 the following equilibrium temperatures at 12 mbar (bottom, hydration) and 16 mbar (top, dehydration) are:

$$SrCl_2 \cdot 6H_2O \underset{28^\circ C}{\overset{33^\circ C}{\rightleftarrows}} SrCl_2 \cdot 2H_2O \underset{44^\circ C}{\overset{48^\circ C}{\rightleftarrows}} SrCl_2 \cdot H_2O \underset{80^\circ C}{\overset{86^\circ C}{\rightleftarrows}} SrCl_2 \quad \text{(Rx.2)}$$

Considering the 6-1 transition, the maximum hydration temperature at 12 mbar is 28 °C, despite monohydrate transitioning to dihydrate at 44 °C. It is because only part of the energy is stored in this transition, and if we want to access all of it, we need to ensure complete conversion from dihydrate to hexahydrate, which releases heat at lower temperatures. Correspondingly, the minimum dehydration temperature for the 6-1 transition is 48 °C as all dihydrate has to be dehydrated to monohydrate to charge the system fully, and this will not occur at

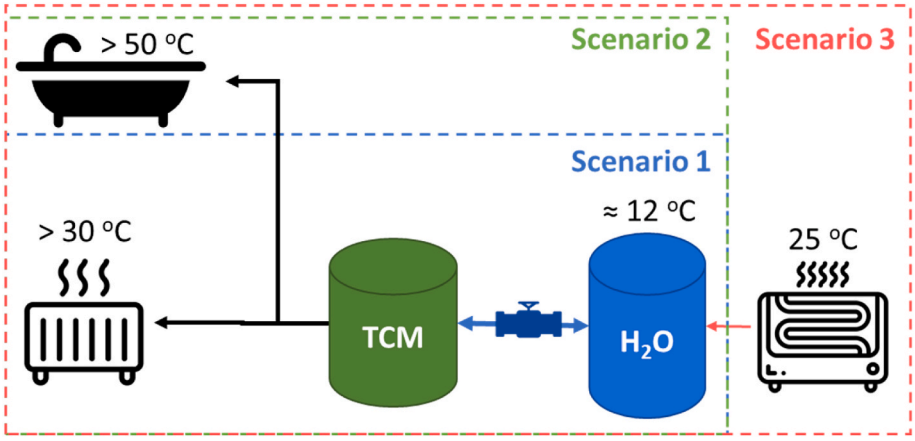

Fig. 5. Summary of use case scenarios indicating temperature requirements of an end-use application and water reservoir temperature with and without temperature boost.

temperatures below 48 °C.

3.3. Energy density filter

In addition to suitable reaction temperature, the amount of energy a material can store is also crucial. TCMs get often praised for their high energy density compared to other heat storage materials [52,53]. Still, there is a large spread between the materials. Early works aimed at providing seasonal TCHS, but in recent years it became evident that this will not be economically feasible with the current technology. Instead, the focus has shifted toward intermittent heat storage that should synchronise heat supply and demand.

To estimate the energy required, we look at an example of heat consumption in Western Europe. The consumption per household is estimated at approximately 45 GJ/year [51]. Therefore, a material with an energy density of 1 GJ/m^3 would enable the design of a compact energy storage system that could buffer a weekly energy demand or be scaled up to a system with higher capacity. A similar energy density criterion has been suggested in an earlier study [12].

3.4. Stability filter

Lastly, we evaluate material stability under reaction conditions. We have excluded salts that are well known to be chemically unstable and to readily degrade in the atmosphere or during repetitive hydration-dehydration cycles [27]. Salts that are highly hygroscopic with a low deliquescence point (below 10% RH) and salts with a low melting point that fulfil the remaining criteria are listed in a separate category. By low melting point, we mean salt hydrates that would melt during hydration or dehydration. Salts that melt below room temperature of 25 °C are completely excluded. The reason for this is the need for additional stabilisation to prevent the agglomeration and performance drop of TCHS [21,52,54], which will most likely impact the energy density and possibly the reaction conditions. Nevertheless, recent progress [52,55,56] in salt hydrate stabilisation opens up new possibilities to use materials that have been previously discarded.

3.5. Theoretical assessment

Materials that have passed the initial screening filters comprise a so-called long list. Salts included in the list were subjected to a theoretical assessment through a literature survey. The survey aimed to uncover additional points for consideration not identified in the Elemental filter, availability, physical stability issues and potential deviations from calculated equilibrium temperatures based on earlier studies. The survey scanned earlier journal publications, material safety data sheets to determine the dangers involving using particular compounds, and USGS reports [57] to evaluate potential scarcity issues.

3.6. Experimental verification

Materials that have passed all the screening filters and the theoretical assessment have been subjected to experimental verification. Readily available salts supplied by the manufacturer. If the procurement of salt was difficult, it was synthesised in the lab, and the composition was verified with powder x-ray diffraction. All samples were pulverised using a pestle and mortar and sieved between 50 and 164 μm fraction.

The experimental verification included the following steps:

1. Synthesised salts were first analysed in ambient conditions in a Miniflex Rigaku powder diffractometer (Cu K α source with a Kβ filter). The measurements were conducted in the 20-60^o 2 θ range at a scan speed of 4°/min and a step size of 0.01^o. Then, the recorded XRD patterns were compared in PDXL software with entries from the Crystallography Open Database (COD) and the Inorganic Crystal Structure Database (ICSD).
2. Reaction reversibility and reaction kinetics were probed in a thermogravimetric analyser (TGA) TGA3+ (Mettler-Toledo). The temperature of TGA was calibrated using the heat flow signal of melting points of naphthalene, In and Zn. The device was equipped with a CellKraft humidifier calibrated by determining the deliquescence onset point at 25 °C of $LiCl{\cdot}H_2O$, $MgCl_2{\cdot}6H_2O$, $K_2CO_3{\cdot}1.5H_2O$ and $Mg(NO_3)_2{\cdot}6H_2O$ [24]. All experiments were conducted under an N_2 atmosphere with a 300 mL/min flow rate. Approximately 5 mg of the ground and sieved sample was loaded in a 40 μL Al pan. Hydration was conducted at 25 °C with a dwell time of 4 h. The dehydration temperature varied between 50 and 170 °C and had a dwell time of 3 h. Ramping speed of 1 K/min between the dwell steps was used for all measurements. The measurements were conducted at isobaric conditions of 12 or 16 mbar. An example of such measurement is given in Fig. 6, showing material with poor reversibility.
3. Finally, the energy storage density was probed by measuring the dehydration enthalpy with differential scanning calorimetry (DSC) in DSC822e (Mettler Toledo). The device was calibrated using melting points of naphthalene, benzophenone, In and Zn. Ground and sieved samples were loaded into a 40 μL Al pan and fully hydrated ex-situ in a desiccator with a saturated salt solution providing fixed relative humidity. The DSC measurement was conducted between 0 and 160 °C, at a scanning rate of 1K/min and an initial dwell time of 15 min at 0 °C. Dry N_2 with a flow rate of 1.4 L/min was used in the measurement.

4. Results of the screening

4.1. Evaluation of the database and the screening filters

This study evaluated 454 unique salt hydrates, 1073 unique reactions and a total of 1336 reactions, summarised in Fig. 7. The vast majority of the reactions have a T_{eq} between 0 and 100 °C, for p_{vap} between 0 and 31 mbar, which is why salt hydrates are favoured for low-temperature applications. For the particular case of 12 mbar p_{vap}, the average $T_{eq,12}$ is 76 °C, and 61.5% of the reactions have $T_{eq,12} < 100$ °C. We evaluated the average T_{eq} between 6 and 31 mbar (0–25 °C), which varies between 55 and 102 °C. It shows that even at low water reservoir temperatures, there are reactions that could potentially provide DHW.

The mean energy density of the entries gathered in the database is 1.58 GJ/m^{3,} and 68% of all reactions have an energy density higher than 1 GJ/m^3. As shown in Fig. 7b, the energy density of the material is relatively insensitive to T_{eq}. Only when considering $\epsilon_V > 3$ GJ/m^3 the average T_{eq} increases to above 100 °C. It means that the operating conditions do not influence the potential storage density of the system.

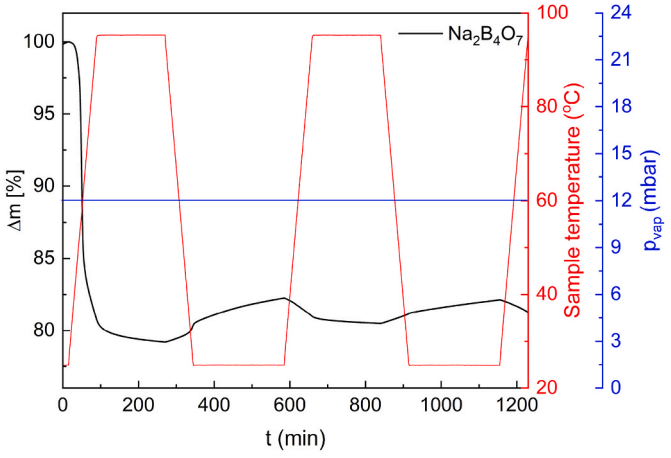

Fig. 6. An example of a TGA screening measurement performed on $Na_2B_4O_7$ at a fixed vapour pressure of 12 mbar (blue line), between 100 and 25 °C (red plot). The measured mass changes are plotted in black.

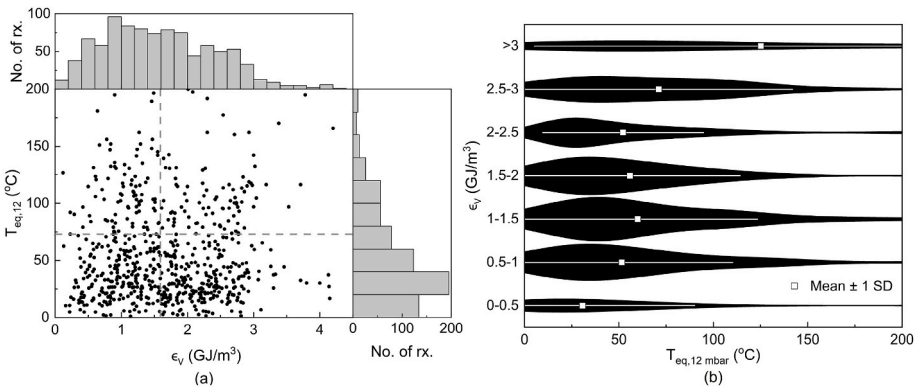

Fig. 7. a) Overview of the entries in the database between 0 and 200 °C with T_{eq} calculated for $p_{vap} = 12$ mbar and the mean values marked with the dashed lines and b) Distribution of $T_{eq,12}$ in different ϵ_V regimes. The white squares show the mean value of the entries, while the white line indicates the standard deviation of the mean value. Reactions exceeding the 0–200 °C range are not included in this representation to improve the readability of the figure.

Combining both factors results in a large pool of potential TCM candidates.

In Fig. 8, we evaluate the reactions gathered in the database with energy density and T_{eq} in mind, as those are based on intrinsic salt properties governed by thermodynamics. Here, we see that about 43% of the reactions fulfil the criteria of the domestic application. In general, there is a linear relationship between hydration and dehydration temperatures for single-step reactions. Nevertheless, in the 0–200 °C region, there is a cluster of data points mainly due to the spread between the maximum hydration and minimum dehydration temperature for a multi-step process, as described in Section 3.2. Fig. 8b shows that most reactions have an energy density of 0.8–2.0 GJ/m^3.

Nevertheless, the distribution of potential reactions is comparable between the three scenarios. Most reactions fulfil Scenario 1, which has the widest temperature range. The impact of minimum hydration temperature is very well visible in Fig. 8c. Here we see that the operating temperature window has a much stronger impact on the material availability than the energy density. Here we also see that a significantly large proportion of reactions has T_{eq} below 30 °C, which could be interesting for cold storage or air conditioning applications. The increase in minimum hydration temperature from 30 to 55 °C results in an approximately 25% decrease in the number of possible reactions. On the contrary, the increase of water source temperature from 10 to 25 °C (12–31 mbar) results in a 40% increase in the number of potential reactions compared to Scenario 2 or 3.5% compared to Scenario 1.

Having discussed the characteristics of collected salts, we look at the entire screening process, summarised in Fig. 9. About 40% of the entries were deemed unsuitable for domestic applications due to their toxicity or availability (Elemental filter). Further, 21% of reactions were rejected because T_{eq} fell outside the 30–160 °C region (Use case scenario filter). It includes reactions where $T_{eq,12} < 30$ °C or $T_{eq,31} < 55$ °C, which is too low for DSH but could be utilized in air conditioning applications [58], and $T_{eq} > 160$ °C, which could be considered for high-temperature applications [20]. Furthermore, about 11.5% of the reactions have energy densities below 1 GJ/m^3, making them undesirable for long-term energy storage applications (Energy density filter). A further 8% of all the entries have been rejected due to stability issues or reaction properties, such as reaction reversibility, formation of polymorphs, melting, and chemical degradation (Stability filter). Nevertheless, some salts are considered for heat storage applications as phase change materials where energy is stored in latent heat instead [59]. It means that nearly 82% of all reactions were rejected in the initial screening and were not included in the long list.

4.2. Theoretical assessment of the long list

The 262 reactions that passed all four screening filters make up the long list subjected to further literature study. Based on our research, we can group the materials into several families listed in Table 2.

The first family, chlorates, nitrates, iodates, and hydroxides, were rejected due to chemical stability issues. The first four clusters are oxidising and potentially explosive [20], which poses a significant risk if large volumes of the material are used for heat storage. Hydroxides were rejected due to their highly alkaline nature, which is very aggressive for many materials considered for the reactor. Moreover, many of the higher hydrates of hydroxide salts have low melting points, making them undesirable for TCHS but possibly interesting for latent heat storage [62]. Finally, although some of the low-temperature hydration reactions have been considered for TCHS, investigated materials have shown a tendency to form carbonates when in contact with moist air,

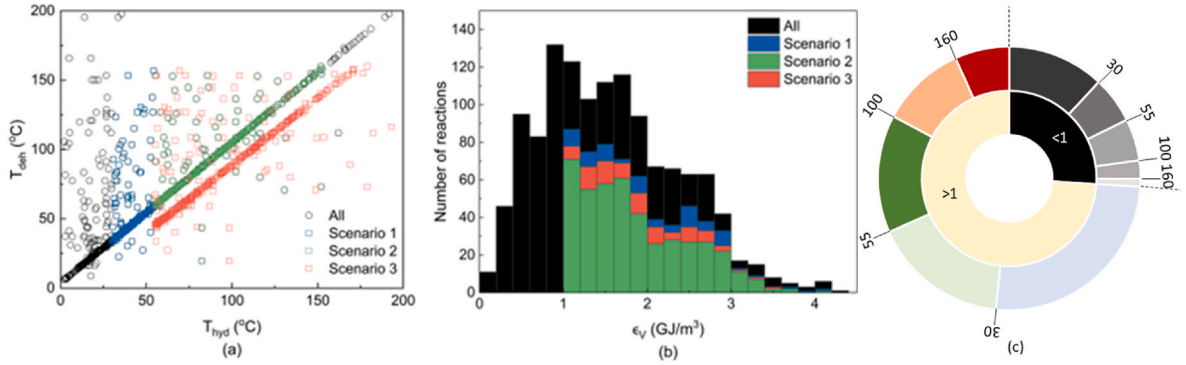

Fig. 8. a) Relationship between hydration temperature at 12/31 mbar and dehydration temperature at 16 mbar b) Number of reactions fitting specific scenario and in a given ϵ_V range c) Distribution of the number of reactions based on ϵ_V (inner ring) and $T_{eq,12}$ (outer ring).

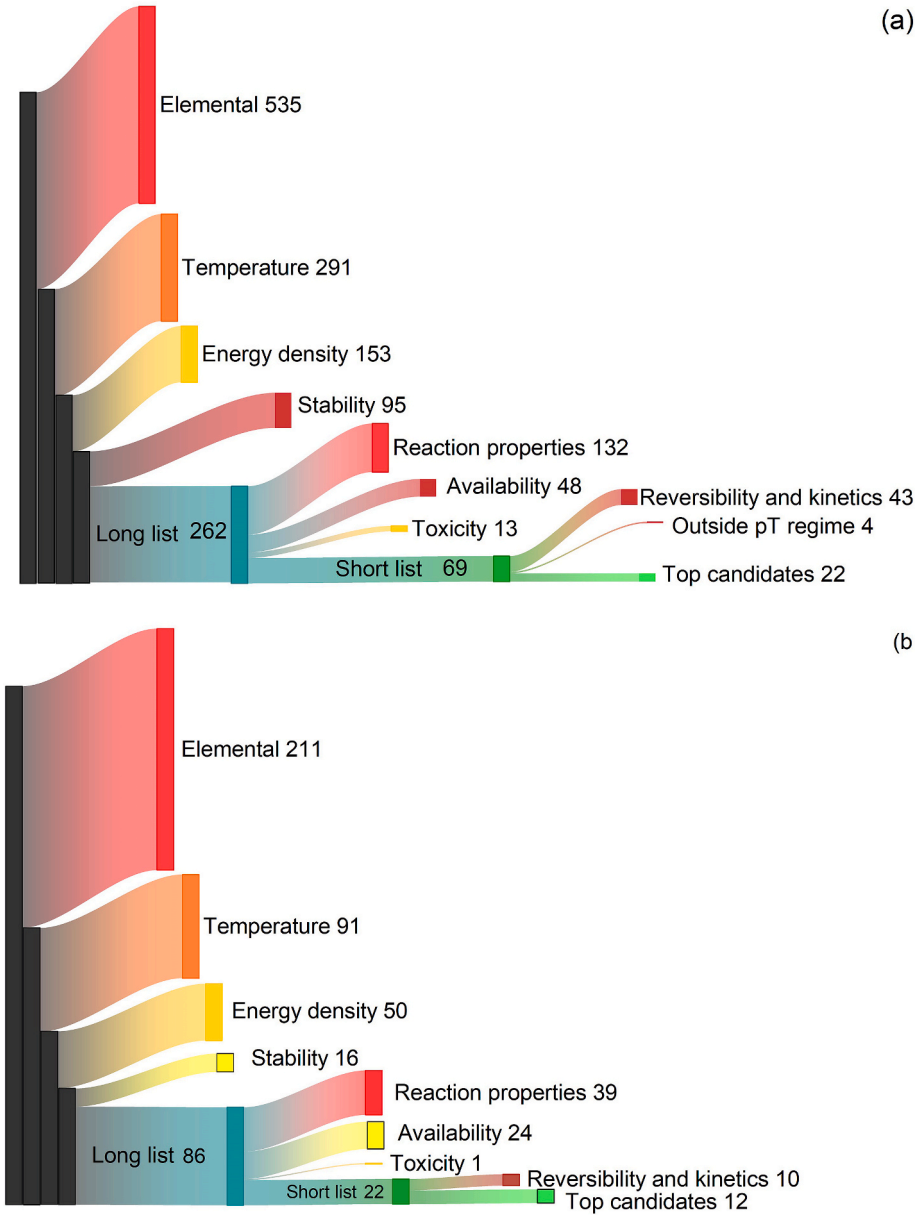

Fig. 9. A Sankey diagram illustrating the impact of screening filters on a) the number of reactions and b) the number of salts applicable for domestic TCHS. Salts with numerous hydration states can be excluded for several reasons, depending on which transition is considered. Here we consider only one of those exclusion factors, as the goal is to give an impression of the number of available salts throughout the screening process.

Table 2
Material families rejected during the theoretical assessment.

	Reason for exclusion	Material family	No. of rejections	Ref
I	Chemically unstable	ClO_4^-, NO_3^-, NO_2^- IO_3^-, OH^-	31	[20,27, 60]
II	Reaction reversibility issues	PO_4^{3-}, BO_2^-	10	[11,20, 21]
III	Price and availability	Cs, Hf, Rb, V, Mo,	30	[61]

reducing the material's energy density [27,60].

The second family of materials consists of phosphates and borates, which are known for poor reaction kinetics and reversibility issues [11, 20]. Although there are some exceptions, such as $CaZn_2(PO_4)_2$ [63], a recent study by Clark et al. [21] supports the earlier observations of slow hydration reaction [18,20]. For a well-performing system, fast reaction kinetics are crucial to ensure high power output.

The final family includes elements that are not commonly considered rare, but through our study of geological survey reports, we have considered being too scarce for large-scale applications. In many cases, the production of compounds with those elements is limited, so they are often considered speciality chemicals.

Other salt hydrates belong to different material families and can be grouped based on their stability, scarcity and reaction properties determined in earlier studies (summarised in Table 3). First, we have materials whose measured dehydration temperature lies above our predefined maximum of 160 °C, although calculated T_{eq} is well within use case scenarios. Second, many salt hydrates are unstable under hydration and/or dehydration conditions. It includes the formation of polymorphs that do not hydrate, decomposition and release of toxic gasses such as HBr or HCl, and melting or formation of an amorphous phase upon dehydration. Third, a group of salts, many of which were considered for TCHS applications under different operating conditions

Table 3
Summary of salt hydrates rejected due to their (thermo)chemical properties and commercial availability.

Reason for exclusion	Salts
$T_{deh} > 160$ °C	$Al_2(OH)_4SO_4$ [11], $Al_2(SO_4)_3$ [64,65], $CaMg((B_3O_4)(OH)_3)_2$ [11], $Fe_{0.66}Fe_4(SO_4)(OH)$ [11], $K_4P_2O_7$ [66], $Mg_3(O_3POB(OH)_3)_2$ [11], MgC_2O_4 [11], $ZrSO_4$ [67]
Unstable under reaction conditions	Al_2O_3 [20], $(Ca_3Fe(OH)_6)_2(SO_4)_3$ [68], $CaCl_2$ [69], $CaNaB_5O_6(OH)_2$ [11], $CaSO_4$ [20], $CuBr_2$ [70], $CuCl_2$ [27], CuF_2 [71], $KMgCl_3$ [72], $MgCl_2$ [26], $Na_2H_2P_2O_7$ [73], Na_2ZnCl_4 [74], $Na_3HP_2O_7$ [73,75], $Na_5P_3O_{10}$ [76], NaCHOO [77], NaCl [78], $NaKC_4H_4O_6$ [79], $ZnCl_2$ [80], ZrF_4 [81]
Poor kinetics under reaction conditions	$Ca_3Al(OH)_6]_2(CO_3)_3$ [82], $Ca_5Si_6O_{17}$ [83], $CaAlSi_2O_8$ [11], $CaSO_4$ [20], $CuSO_4$ [84], $Fe(SO_4)(OH)$ [85], $KAl(SO_4)_2$ [86], $MgSO_4$ [21], $Na_4P_2O_7$ [87], $ZnSO_4$ [88,89], $X_2Y(SO_4)_2$ and $XAl(SO_4)_2$ (X = Na, K, NH_4; Y=Cu, Fe, Zn, Mg) [11,90–92],
Toxicity	$Cu(HCOO)_2$, $SnBr_4$, $SnCl_4$
Limited commercial availability	$CH_3NH_2Al(SO_4)_2$, $XSiF_6$ X=(Sr, Ca), $K_2CO(SO_4)_2$, Li_2ZnCl_4, $Fe(SO_4)(OH)$, $MgSO_3$, $(NH_2OH)Al(SO_4)_2$

but not fitting our selection criteria. Last, materials considered too toxic to be used in a domestic environment or not commercially available and have no easy ways of synthesising them.

4.2.1. Shortlist

The resulting shortlist contains 22 salts and 69 reactions. In addition, compounds not extensively studied in the literature were subjected to an isobaric test in TGA, described in Section 3.7. The measurement was conducted at 12 or 16 mbar vapour pressure between 25 and 50/170 °C with 1 K/min scanning speed. Based on those screening measurements, 15 salt hydrates were excluded due to reaction irreversibility or poor reaction kinetics. Those compounds are summarised in Table 4.

The first group of salts did not show any mass uptake when exposed to either 12 or 16 mbar at 25 °C despite our thermodynamic calculations suggesting that a hydrate should form. Both zinc salts in the second group showed very slow mass uptake, resulting in partial conversion in the allocated time, which we consider too low for practical application. Third, $MgBr_2$ has shown continuous decomposition during experimental screening. Poor stability in moist conditions was expected as $MgCl_2$ is also prone to decomposition [26]. Next, $K_2C_2O_4$ rehydrated to a lower hydration state than predicted by thermodynamics, which could be caused by large hysteresis in reaction conditions, an error in the thermodynamic data or instability of the higher hydrate under given conditions. Last, we have $SrBr_2$ and $SrCl_2$, for which some of the possible transitions were rejected, as they do not fulfil the use case scenarios despite being fully reversible [23,93]. We have rejected the $SrBr_2$ 1-0 reaction, as to reach the anhydrous phase at 12 mbar, a temperature above 160 °C is needed. It exceeds our use case scenarios. Next, we rejected all reactions involving $SrCl_2{\cdot}6H_2O$ because it cannot provide either DSH at 12 mbar or DHW at 31 mbar.

Table 4
An overview of salt hydrates rejected during experimental screening, the reason for their rejection and the cumulative number of reactions rejected.

Reason for rejection	Salt hydrate	Total no. of rx. rejected
Lack of hydration	AlF_3, Na_2CO_3, $Na_2B_4O_7$, $NaHC_2O_4$, $Sr(HCOO)_2$, $Na_2S_2O_3$,	10
Very poor hydration kinetics	ZnC_2O_4, $Zn(HCOO)_2$	2
Decomposition during measurement	$MgBr_2$,	7
Limited reversibility resulting in $\epsilon_V < 1$ GJ/m^3	$K_2C_2O_4$	1
Reaction conditions outside designated pT region	$SrBr_2$, $SrCl_2$	4

In the end, 8 salts and 9 reactions fulfil all screening criteria. We will discuss those compounds in detail in Section 5.

4.2.2. Salt hydrates commonly investigated for TCHS that did not pass our screening

During our salt hydrate screening, we evaluated hundreds of salts, many of which are under active investigation for low-temperature TCSH but did not pass our screening filters [52,94–96]. Some of the most commonly considered families of materials are sulphates, in particular $MgSO_4$, $ZnSO_4$, $Al_2(SO_4)_3$ and $KAl(SO_4)_2$ [12,69,88,97,98]. All salts are readily available and seem enticing due to their high energy density. Unfortunately, those salts suffer from large reaction hysteresis, poor reaction kinetics and reversibility [18]. As a result, many attempts were made to improve and stabilize those materials and improve reaction kinetics, often at the expense of other properties [99–104].

Within chlorides, $MgCl_2$ and $LaCl_3$ have been extensively investigated. $MgCl_2$ is highly hygroscopic and known to agglomerate and decompose with cycling [26,105–108]. $LaCl_3$ is less known but has been gaining popularity [9,94,109]. Although it has a high energy density and is proven stable under reaction conditions, the material's high cost and hazardous nature are a barrier to a domestic application.

Finally, several lithium salts have been investigated for TCHS [110], from which LiOH [22,60,111] is one of the most popular because of its high energy density (2.2 GJ/m^3, 1.44 MJ/kg) and reversibility at low temperatures. However, the hydration kinetics are very poor. Therefore most of the studies focused on improving those. Additionally, as mentioned in section 4.2, an undesired side reaction with CO_2 is a common issue when working with hydroxides.

5. Most promising candidates

5.1. Materials that do not need stabilisation

In Table 5, we present the results of the final screening. Despite considering over 1073 reactions and experimentally testing 18 salts, our list consists mainly of salts already considered for TCHS applications. The best examples are K_2CO_3 [26,112–118], $SrBr_2$ [94,119–123], $SrCl_2$ [23,124–126], LiCl [30,127–130] and $CaCl_2$ [105,131–135], all of which were studied in their pure form, as a part of a composite or even in a small reactor. Newly considered TCM materials are NaI and $(NH_4)_2Zn(SO_4)_2$. So far, very little work has been done on both materials, but they warrant more attention.

5.1.1. Potassium carbonate

Since the Donkers et al. [22] review, K_2CO_3 has gained much interest in the literature. Its low cost and chemical robustness are the most commonly cited advantages [116] over the other studied materials. However, the material suffers from reaction hysteresis, which some studies have attempted to combat [136–138]. In addition, the material can react with CO_2 in the air [26] and form other compounds that can negatively impact the charging temperature [139]. With a water source of 12 mbar, K_2CO_3 can provide DSH only (Scenario 1). However, it could provide DHW with a water source of 14 mbar or 12 °C [140] (Scenario 3). In either case, dehydration is easily achievable below 100 °C.

5.1.2. Strontium bromide

$SrBr_2$ is one of the most popular TCM candidates due to its high energy density, fast kinetics and (dis)charge temperatures, meeting all domestic needs [52]. $SrBr_2$ 1–6 transition has very narrow hysteresis [121], and there are no reported side reactions. The main disadvantages of this material are its relatively high cost [52] and mechanical stability issues due to large volumetric changes between mono- and hexahydrate [141]. Most recent research focuses on improving salt's heat and mass transfer and its mechanical stability by adding an inert matrix [52,133,142]. The temperature output of $SrBr_2$ is comparable with that of K_2CO_3. At 12 mbar, it can provide DSH only (Scenario 1), and to reach 55 °C, a

Table 5
The most promising candidates for domestic TCHS validated experimentally. The top part of the table details reaction properties at 12 mbar and the bottom part details reaction temperatures at 16 mbar. Price estimates are based on bulk volume prices from Alibaba.com.

Reaction	T_{hyd} (°C)	T_{deh} (°C)	T_{eq} (°C)	ΔH (kJ/mol H_2O)	ϵ_V (GJ/m^3) hyd]	ϵ_G (MJ/kg) hyd]	V $_{H2O}$ (L/GJ)	υ (%)	Cost ($/MJ)	Use case scenario	Ref
K_2CO_3 0–1.5	48.6	73.2	61.7	60.8	1.19	0.55	297	21.7	0.9	1 + 3	[140]
$SrBr_2$ 1-6	42.8	47.5	46.9	54.4	1.87	0.76	332	53.0	4.2	1 + 3	[121]
$SrCl_2$ 0-1	59.7	109.8	80.3	63.0	1.04	0.36	287	14.1	2.2	1–3	[23]
$SrCl_2$ 0-2	34.5	109.8	N/A	61.5	1.73	0.63	294	27.1	1.3	1 + 3	[23]
LiCl 0-1	61.7	66.4	66.1	53.8	1.57	0.89	335	40.9	73.0	1–3	[26]
CaC_2O_4 0-1	129.6	132.5	133.8	66.7	1.00	0.46	271	9.0	21.7	1–3	This study
NaI 0-2	39.6	43.5	40.9	56.2	1.50	0.60	320	42.2	1.4	1 + 3	This study
$NaCH_3COO$ 0-3	31.3	36.3	33.6	41.9	1.34	0.93	432	42.8	1.0	3	This study
$(NH_4)_2Zn(SO_4)_2$ 0-6	34.4	40.0		55.0	1.58	0.82	327		0.7[a]	3	This study

[a] Estimate based on prices of $(NH_4)_2SO_4$ and $ZnSO_4{\cdot}H_2O$.

water source with approximately 24.8 mbar (21 °C) is required (Scenario 3) [121]. Nevertheless, charging is readily attainable below 100 °C.

5.1.3. Strontium chloride

$SrCl_2$ is not as popular as $SrBr_2$ but has been investigated with H_2O [23,124–126] and NH_3 [143–145] as the reactive gas. Although many hydration states give an impression of substantial flexibility in the design of operating conditions, most reactions have considerable hysteresis and poor reaction kinetics, which impose substantial limitations [23]. The high energy density of $SrCl_2{\cdot}6H_2O$ is commonly cited in its favour, despite the relatively low melting point of hexahydrate (61.3 °C), which could have adverse effects on material stability [124–126] and the need for high vapour pressures during hydration to reach desired output temperature [23,146]. Similarly to $SrBr_2$, an inert matrix has been proposed to overcome mechanical stability issues, achieved at the expense of energy density [125]. Finally, similarly to $SrBr_2$, material cost is substantial compared to other proposed salts.

5.1.4. Lithium chloride

LiCl has been studied for TCHS applications primarily as a part of a composite material due to its low deliquescence point (11% RH at 25 °C [24]). Because of that, some applications used both hydration-dehydration transition and deliquescence [147] as it increases energy density and the operating window. This also means that LiCl will most likely require some form of stabilisation by, for example, impregnation to limit the challenges related to its high hygroscopicity. Its narrow reaction hysteresis, high hydration temperatures and high energy density make it a good candidate for TCHS [26]. It can readily provide temperatures high enough for DHW at 12 mbar (Scenario 2) and dehydrate below 100 °C. The main disadvantage of LiCl is its high cost, as lithium is one of the critical elements [38], whose prices have steadily increased in the last years [148] due to increasing demand for Li-batteries.

5.1.5. Calcium oxalate

CaC_2O_4 is a lesser-known salt which has been shown to be stable for at least 100 cycles [149]. However, despite very narrow reaction hysteresis and high hydration temperatures easily covering DHW demand (Scenario 2), its operating conditions are at the boundary between low and high-temperature applications, which is most likely why it did not gain any traction with either of the applications [150]. The main disadvantages of this material involve its relatively low energy density and high price and toxicity compared to other salt hydrates.

5.1.6. Sodium acetate

$NaCH_3COO$ is well known in the heat storage world as a phase change material (PCM) since the trihydrate melts at about 58 °C [151–154]. Nevertheless, to the best of our knowledge, it was not studied as a TCM. The large reaction hysteresis and the low melting point of the trihydrate pose challenges for DHW generation. Moreover, to reach DHW temperatures, the vapour pressure of 72 mbar (39.5 °C) has to be supplied, which is higher than what we have predefined in Scenario 3. For this application, NaI would also require some form of stabilisation to mitigate the melting of its hydrate. Nevertheless, the low material cost and adequate energy density could make it a contender for DSH applications.

5.1.7. Sodium iodide

NaI is a readily available material with a satisfactory energy density. At 12 mbar, it can easily provide DSH. To reach DHW temperatures, a vapour pressure of approximately 22 mbar (19 °C) is needed. However, the dihydrate has a relatively low melting point which could be challenging in this application without added stabilisation. The main disadvantages of this material are its sensitivity to light and moisture, which can lead to its chemical degradation and formation of toxic products during storage, handling and operation.

5.1.8. Ammonium zinc sulphate

$(NH_4)_2Zn(SO_4)_2$ and other Tutton salts [90,155,156] have been recently brought to the attention of the researchers, but there is very little work done on those materials. A recent study has shown that ammonium zinc sulphate is one of the very few salts in this family that is fully reversible and stable over at least 10 cycles [90]. The possible disadvantage of this material is decomposition with prolonged cycling as some other salts in $(NH_4)_2X(SO_4)_2$ (where *X* stands for divalent metal cation) family have shown loss of ammonia over time. From an application point of view, the material does not seem commercially available in large quantities, which would increase the storage cost. It could be synthesised from cheap precursors (for example $(NH_4)_2SO_4$, and $ZnSO_4$) or by using spent galvanising electrolyte [157]. Nevertheless, the potentially high cost of material synthesis optimisation introduces new risks. In our evaluation, we have confirmed that this material could provide DSH with a water source at 16 mbar, which is above the conditions of Scenario 1 and could potentially fulfil the conditions of Scenario 3.

5.2. Materials that require stabilisation

Data for the salts summarised in Table 6 that fulfil all the criteria but are highly hygroscopic or have a low melting point were not verified experimentally as they need to be stabilized first to test the validity of the thermodynamic calculations. In recent years, much work has been done on stabilising salt hydrates to enhance their mechanical stability

Table 6
The most promising candidates for domestic TCHS where stabilisation is mandatory. The theoretical equilibrium temperature is given at 12 mbar for orientation. Price estimates are based on bulk volume prices from Alibaba.com. The cost of stabilisation is not included.

Reaction	$T_{eq,12}$ (°C)	ΔH (kJ/mol H_2O)	ϵ_V (GJ/m^3)	ϵ_G (MJ/kg)	V_{H2O} (L/GJ)	υ (%)	Cost ($/MJ)	Use case scenario
$CaBr_2$ 6-0	73.8	62.08	2.67	1.20	290	56.5	2.9	1–3
$CaCl_2$ 6-0	34.96	62.5	2.93	2.96	285	59.7	0.03	1
$CaCl_2$ 6-1	34.96	60.4	2.36	1.38	298	55.0	0.07	1
$CaCl_2$ 6-2	34.96	62.8	1.96	1.15	287	37.6	0.08	1
$CaCl_2$ 4-0	41.65	61.1	2.44	1.33	295	48.4	0.07	1 + 3
$CaCl_2$ 4-1	41.65	57.12	1.71	0.94	315	42.4	0.1	1 + 3
$CaCl_2$ 4-2	41.65	60.37	1.21	0.66	298	20.1	0.1	1 + 3
LiBr 2-0	36.86	63.87	2.29	0.92	318	55.7	10.0	1–3
LiBr 2-1	36.86	58.18	1.04	0.47	310	31.0	19.6	1–3
LiBr 1-0	92.38	69.55	1.77	0.66	259	37.0	13.9	1–3
LiCl 2-0	31.94	63.45	2.43	1.62	284	61.2	22.8	1–3
LiCl 2-1	31.94	64.00	1.22	0.82	281	34.3	45.1	1–3
$ZnBr_2$ 2-0	45.52	62.29	1.44	0.48	289	38.0	4.6	1 + 3

and long-term cyclic reversibility [52,55]. This allows us to reconsider previously rejected salts due to handling and agglomeration issues [18]. Additionally, the utilization of the deliquescence transition to compensate for the loss of energy density due to the inert matrix is becoming a popular research topic [56,132,135]. Nevertheless, the matrix that is chosen to stabilize the salt can affect the reaction onset points and the reversibility of the reaction, as there is a chance for chemical interaction between the matrix and the salt [121]. Furthermore, the matrix will also decrease the energy density and increase the cost of the material. For those reasons, the following compounds are presented as theoretically interesting compounds that require further research and validation.

5.2.1. Calcium bromide

Calcium bromide has been considered for heat storage applications in the past, but primarily as a phase change material due to hexahydrate's relatively low melting point [158]. Heat storage utilising the dissolution or deliquescence reaction [159,160] has also been considered due to the low deliquescence point of hexahydrate [24]. The salt readily provides temperatures high enough for DHW, even at low vapour pressures. Based on that, there is a potential for $CaBr_2$ as a TCHS material, provided a suitable encapsulation method is found. Nevertheless, as with many other halide salts, care must be taken so that no hydrolysis occurs because this will lead to toxic and corrosive gasses forming.

5.2.2. Calcium chloride

Calcium chloride is a very common compound that has been intensively studied both as TCM and PCM. The early work on $CaCl_2$ as TCM has shown that the material cannot be used in its pure form due to its high hygroscopicity and a low melting point of its hydrates, leading to agglomeration and performance loss [69]. The more recent work utilizes various stabilisation methods [132] and shows that this material can be used as a TCM, provided a suitable matrix is found. The promising outlook for this salt is further supported by fast reaction kinetics and its favourable price. If all hydration states are utilized, and possibly the deliquescence transition as well, then only DHS can be provided. By sacrificing part of the energy density, hot tap water could be provided at elevated vapour pressures, provided the melting of the lower hydrates is mitigated.

5.2.3. Lithium bromide

Lithium bromide is an extremely hygroscopic compound with a DRH of 6.4% [24] and thus never used in its pure form. It has been considered for automotive application with methanol as a working gas [161], in absorption systems [162] or as a part of composite [163]. The main recurring drawback of the compound is its high price due to the high lithium demand for electrical batteries [164]. Dihydrate formation could readily provide space heating, and at lower energy densities, DHW could be generated by utilising the 0–1 transition, even at vapour pressures as low as 1 mbar.

5.2.4. Zinc bromide

$ZnBr_2$ is already widely used in energy storage as a main electrolyte component in $ZnBr_2$ redox flow batteries [165]. Nevertheless, it hasn't been applied for heat storage applications. Similarly to LiBr, $ZnBr_2$ has a very low DRH [24], and its hydrate has a low melting point [33]. It can readily provide DHS, but production of DHW would require a vapour pressure of at least 16 mbar.

6. Conclusion and outlook

In this work, we have evaluated 1073 reactions and 454 salt hydrates in view of domestic thermochemical heat storage. Reactions that passed the initial screening made up the long list of 261 reactions subjected to a theoretical assessment. This assessment revealed that only a shortlist of 69 reactions is worthwhile to test experimentally. In the end, only 8 salts (K_2CO_3, $SrBr_2$, $SrCl_2$, NaI, CaC_2O_4, $NaC_2H_3O_2$, $(NH_4)_2Zn(SO_4)_2$, LiCl) and 9 reactions have shown to fulfil all the essential criteria. Additional 4 salts ($CaBr_2$, $CaCl_2$, LiBr, $ZnBr_2$) and 13 reactions are promising, provided a suitable stabilisation method is applied to prevent their mechanical disintegration during operation. Of those compounds, only 3 (NaI, $(NH_4)_2Zn(SO_4)_2$, $ZnBr_2$) have not been extensively researched for TCHS applications. It shows that the number of salt hydrates that could be used for domestic heat storage is quite limited, and there are two primary reasons for that. First of all, the operating window for domestic applications is very narrow. Even in the most relaxed case, Scenario 3, we have considered a temperature range of 130 °C and a vapour pressure range of 15 mbar, which poses many restrictions. Secondly, although reaction enthalpies and entropies for many reactions are relatively similar, the p-T relationship strongly depends on enthalpy. It means that even minor changes in the enthalpy lead to significant shifts in reaction conditions.

Future work has two major outlooks. Firstly, the shortlisted materials should be evaluated on a larger scale by testing the (de)hydration behaviour on a particle scale and even in small reactors. In this evaluation, the long-term mechanical and chemical stability should be investigated, and reaction kinetics closely monitored. Thermal conductivity measurements could also expand the material evaluation to gain even more insight into material properties. Secondly, future material screening works should venture outside the tabulated values to increase the pool of candidates. For example, the thermodynamic properties of readily available compounds that are not yet reported in the literature should be measured to assess those compounds better. Additionally, numerical modelling such as DFT and machine learning could be employed to predict the stability of new (double)salts and their thermodynamic properties.

CRediT authorship contribution statement

Natalia Mazur: Conceptualization, Methodology, Validation,

Investigation, Writing – original draft. **Melian A.R. Blijlevens:** Validation, Investigation, Writing – original draft. **Rick Ruliaman:** Conceptualization, Methodology, Validation, Investigation. **Hartmut Fischer:** Conceptualization, Methodology, Investigation, Writing – review & editing, Supervision, supervision. **Pim Donkers:** Conceptualization, Methodology. **Hugo Meekes:** Writing – review & editing, Supervision. **Elias Vlieg:** Writing – review & editing, Supervision. **Olaf Adan:** Conceptualization, Methodology, Investigation, Writing – review & editing, Supervision, supervision. **Henk Huinink:** Conceptualization, Methodology, Investigation, Resources, Writing – review & editing, Supervision, Project administration, Funding acquisition.

Declaration of competing interest

The authors declare that they have no known competing financial interests or personal relationships that could have appeared to influence the work reported in this paper.

Data availability

Data will be made available on request.

Acknowledgements

This publication is part of the project Mat4Heat with project number 739.017.014 of the research program Mat4Sus which is financed by the Dutch Research Council (NWO).

Appendix A. Supplementary data

Supplementary data to this article can be found online at https://doi.org/10.1016/j.renene.2023.119331.

References

[1] IRENA - Statistics Time Series n.d. https://www.irena.org/Statistics/View-Data-by-Topic/Capacity-and-Generation/Statistics-Time-Series (accessed July 6, 2022)..
[2] P.A.J. Donkers, Experimental Study on Thermochemical Heat Storage Materials, Technische Universiteit Eindhoven, 2015.
[3] IEA n.d. https://www.iea.org/regions/europe (accessed March 23, 2022)..
[4] Energy consumption in households n.d. https://ec.europa.eu/eurostat/statistics-explained/index.php?title=Energy_consumption_in_households (accessed March 23, 2022).
[5] L. Scapino, H.A. Zondag, J. Van Bael, J. Diriken, C.C.M. Rindt, Sorption heat storage for long-term low-temperature applications: a review on the advancements at material and prototype scale, Appl. Energy 190 (2017) 920–948, https://doi.org/10.1016/j.apenergy.2016.12.148.
[6] P. Donkers, L. Pel, M. Steiger, O. Adan, Deammoniation and ammoniation processes with ammonia complexes, AIMS Energy 4 (2016) 936–950, https://doi.org/10.3934/energy.2016.6.936.
[7] A. Calderón, C. Barreneche, K. Hernández-Valle, E. Galindo, M. Segarra, A. I. Fernández, Where is Thermal Energy Storage (TES) research going? – a bibliometric analysis, Sol. Energy 200 (2020) 37–50, https://doi.org/10.1016/j.solener.2019.01.050.
[8] N. Yu, R.Z.Z. Wang, L.W.W. Wang, Sorption thermal storage for solar energy, Prog. Energy Combust. Sci. 39 (2013) 489–514, https://doi.org/10.1016/j.pecs.2013.05.004.
[9] K.E. N'Tsoukpoe, T. Schmidt, H.U. Rammelberg, B.A. Watts, W.K.L. Ruck, A systematic multi-step screening of numerous salt hydrates for low temperature thermochemical energy storage, Appl. Energy 124 (2014) 1–16, https://doi.org/10.1016/j.apenergy.2014.02.053.
[10] A.J. Carrillo, J. González-Aguilar, M. Romero, J.M. Coronado, Solar energy on demand: a review on high temperature thermochemical heat storage systems and materials, Chem. Rev. 119 (2019) 4777–4816, https://doi.org/10.1021/acs.chemrev.8b00315.
[11] S. Afflerbach, R. Trettin, A systematic screening approach for new materials for thermochemical energy storage and conversion based on the Strunz mineral classification system, Thermochim. Acta 674 (2019) 82–94, https://doi.org/10.1016/j.tca.2019.02.010.
[12] K. Visscher, J.B.J. Veldhuis, H.a.J. Oonk, PJ Van Ekeren, J.G. Blok, Compacte Chemische Seizoensopslag Van Zonnewarmte, 2004.
[13] H.A. Zondag, VM Van Essen, P.W. Bach, M. Bakker, An evaluation of the economical feasibility of seasonal sorption heat storage, in: 5th Int Renew Energy Storage Conf IRES, 2010, pp. 22–24.
[14] F. Trausel, A.J. De Jong, R. Cuypers, A review on the properties of salt hydrates for thermochemical storage, Energy Proc. 48 (2014) 447–452, https://doi.org/10.1016/j.egypro.2014.02.053.
[15] M. Deutsch, D. Müller, C. Aumeyr, C. Jordan, C. Gierl-Mayer, P. Weinberger, et al., Systematic search algorithm for potential thermochemical energy storage systems, Appl. Energy 183 (2016) 113–120, https://doi.org/10.1016/j.apenergy.2016.08.142.
[16] T. Yan, R.Z. Wang, T.X. Li, L.W. Wang, I.T. Fred, A review of promising candidate reactions for chemical heat storage, Renew. Sustain. Energy Rev. 43 (2015) 13–31, https://doi.org/10.1016/j.rser.2014.11.015.
[17] E. Laurenz, L. Schnabel, G. Fuldner, Assessment of thermodynamic equilibrium properties of salt hydrates for heat transformation applications at different temperature levels Eric Laurenz , Gerrit Füldner , Lena Schnabel, Heat Powered Cycles Conf. (2016).
[18] P.A.J. Donkers, L.C. Sögütoglu, H.P. Huinink, H.R. Fischer, O.C.G. Adan, A review of salt hydrates for seasonal heat storage in domestic applications, Appl. Energy 199 (2017) 45–68, https://doi.org/10.1016/j.apenergy.2017.04.080.
[19] S. Kiyabu, J.S. Lowe, A. Ahmed, D.J. Siegel, Computational screening of hydration reactions for thermal energy storage: new materials and design rules, Chem. Mater. 30 (2018), https://doi.org/10.1021/acs.chemmater.7b05230, 2006–17.
[20] M. Richter, E.M. Habermann, E. Siebecke, M. Linder, A systematic screening of salt hydrates as materials for a thermochemical heat transformer, Thermochim. Acta 659 (2018) 136–150, https://doi.org/10.1016/j.tca.2017.06.011.
[21] R.J. Clark, G. Gholamibozanjani, J. Woods, S. Kaur, A. Odukomaiya, S. Al-Hallaj, et al., Experimental screening of salt hydrates for thermochemical energy storage for building heating application, J. Energy Storage 51 (2022), 104415, https://doi.org/10.1016/J.EST.2022.104415.
[22] M. Kubota, S. Matsumoto, H. Matsuda, H.Y. Huang, Z.H. He, X.X. Yang, Chemical heat storage with LiOH/LiOH·H2O reaction for low-temperature heat below 373 K, Adv. Mater. Res. 953–954 (2014) 757–760, https://doi.org/10.4028/WWW.SCIENTIFIC.NET/AMR.953-954.757.
[23] M.A.R. Blijlevens, N. Mazur, W. Kooijman, H.R. Fischer, H.P. Huinink, H. Meekes, et al., A study of the hydration and dehydration transitions of SrCl2 hydrates for use in heat storage, Sol. Energy Mater. Sol. Cells 242 (2022), 111770, https://doi.org/10.1016/j.solmat.2022.111770.
[24] L. Greenspan, Humidity fixed points of binary saturated aqueous solutions, J. Res. Natl. Bur Stand. A Phys. Ics. Chem. 82A (1976) 89–96.
[25] L.J. Mauer, L.S. Taylor, Water-solids interactions: deliquescence, Annu. Rev. Food Sci. Technol. 1 (2010) 41–63, https://doi.org/10.1146/annurev.food.080708.100915.
[26] L.C. Sögütoglu, P.A.J. Donkers, H.R. Fischer, H.P. Huinink, O.C.G. Adan, In-depth investigation of thermochemical performance in a heat battery: cyclic analysis of K2CO3, MgCl2and Na2S, Appl. Energy 215 (2018) 159–173, https://doi.org/10.1016/j.apenergy.2018.01.083.
[27] L.C. Sögütoglu, Fundamentals of Salt Hydration for Heat Battery Application, Eindhoven university of technology, 2020.
[28] M. van Essen, L.P.J. Bleijendaal, B.W.J. Kikkert, H.A. Zondag, M. Bakker, P. W. Bach, Development of a compact heat storage system based on salt hydrates, Int. Conf. Sol. Heating, Cool. Build. (2010) 1–8, https://doi.org/10.18086/eurosun.2010.16.37.
[29] M.A.J.M. Beving, A.J.H. Frijns, C.C.M. Rindt, D.M.J. Smeulders, Effect of cycle-induced crack formation on the hydration behaviour of K2CO3 particles: experiments and modelling, Thermochim. Acta 692 (2020), 178752, https://doi.org/10.1016/j.tca.2020.178752.
[30] L. Calabrese, V. Brancato, V. Palomba, A. Frazzica, L.F. Cabeza, Innovative composite sorbent for thermal energy storage based on a SrBr2·6H2O filled silicone composite foam, J. Energy Storage 26 (2019), 100954, https://doi.org/10.1016/j.est.2019.100954.
[31] L. Glasser, Thermodynamics of inorganic hydration and of humidity control, with an extensive database of salt hydrate pairs, J. Chem. Eng. Data 59 (2014) 526–530, https://doi.org/10.1021/je401077x.
[32] Washburn EW. International Critical Tables of Numerical Data, Physics, Chemistry and Technology (1st Electronic Edition) n.d..
[33] V.S. IVSY. Database of Thermal Constants of Substances n.d. http://www.chem.msu.ru/cgi-bin/tkv.pl?brutto=&show=search&joules=0 (accessed May 11, 2022)..
[34] Tchounwou PB, Yedjou CG, Patlolla AK, Sutton DJ. Heavy Metals Toxicity and the Environment n.d. https://doi.org/10.1007/978-3-7643-8340-4_6..
[35] Occupational Safety and Health Administration, Toxic Metals, Occupational Safety and Health Administration, 2004.
[36] Lenntech. Heavy Metals n.d.
[37] G.B. Haxel, J.B. Hedrick, Rare earth elements—critical Resources for high technology, US Geological Survey 87 (2) (2002).
[38] A.J. Hurd, R.L. Kelley, R.G. Eggert, M.H. Lee, Energy-critical elements for sustainable development, MRS Bull. 37 (2012) 405–410, https://doi.org/10.1557/MRS.2012.54.
[39] N. Hatada, K. Shizume, T. Uda, Discovery of Rapid and Reversible Water Insertion in Rare Earth Sulfates : A New Process for Thermochemical Heat Storage, vol. 1606569, 2017, pp. 1–6, https://doi.org/10.1002/adma.201606569.
[40] K. Shizume, N. Hatada, S. Yasui, T. Uda, Multi-step hydration/dehydration mechanisms of rhombohedral Y2(SO4)3: a candidate material for low-temperature thermochemical heat storage, RSC Adv. 10 (2020) 15604–15613, https://doi.org/10.1039/d0ra02566f.
[41] C. Geelen, L. Krosse, P. Sterrenburg, E.-.J. Bakker, N. Sijpheer, Handboek Energiepalen, 2003, p. 20.

[42] L.F. Cabeza, Advances in Thermal Energy Storage Systems: Methods and Applications, Woodhead Publishing, 2021, https://doi.org/10.1016/B978-0-12-819885-8.00002-4.

[43] K.E. N'Tsoukpoe, N. Mazet, P. Neveu, The concept of cascade thermochemical storage based on multimaterial system for household applications, Energy Build. 129 (2016) 138–149, https://doi.org/10.1016/j.enbuild.2016.07.047.

[44] Solar Keymark n.d. http://www.solarkeymark.nl/DBF/(accessed July 7, 2022).

[45] F. Kuznik, K. Johannes, Thermodynamic efficiency of water vapor/solid chemical sorption heat storage for buildings: theoretical limits and integration considerations, Appl. Sci. 10 (2020) 489, https://doi.org/10.3390/app10020489.

[46] G. Martínez-Rodríguez, A.L. Fuentes-Silva, M. Picón-Núñez, Targeting the maximum outlet temperature of solar collectors, Chem. Eng. Trans. 70 (2018) 1567–1572, https://doi.org/10.3303/CET1870262.

[47] B.W. Olesen, Radiant Floor Heating in Theory and Practice, vols. 19–24, 2002.

[48] J. Bartram, Y. Chartier, J.V. Lee, K. Pond, S. Surman-Lee (Eds.), Legionella and the Prevention of Legionellosis, 2007.

[49] Lower Water Heating Temperature n.d. https://www.energy.gov/energysaver/do-it-yourself-savings-project-lower-water-heating-temperature (accessed July 7, 2022).

[50] HSE-Hot and cold water systems n.d. https://www.hse.gov.uk/legionnaires/hot-and-cold.htm (accessed July 7, 2022).

[51] E. Commission, Energy Consumption by End-Use, 2020.

[52] W. Li, J.J. Klemeš, Q. Wang, M. Zeng, Salt hydrate–based gas-solid thermochemical energy storage: current progress, challenges, and perspectives, Renew. Sustain. Energy Rev. 154 (2022), 111846, https://doi.org/10.1016/j.rser.2021.111846.

[53] P. Tatsidjodoung, N. Le Pierrès, L. Luo, A review of potential materials for thermal energy storage in building applications, Renew. Sustain. Energy Rev. 18 (2013) 327–349, https://doi.org/10.1016/j.rser.2012.10.025.

[54] W. Li, M. Zeng, Q. Wang, Development and performance investigation of MgSO4/SrCl2 composite salt hydrate for mid-low temperature thermochemical heat storage, Sol. Energy Mater. Sol. Cells 210 (2020), 110509, https://doi.org/10.1016/j.solmat.2020.110509.

[55] D. Mohapatra, J. Nandanavanam, Salt in matrix for thermochemical energy storage - a review, Mater. Today Proc. 72 (2023) 27–33, https://doi.org/10.1016/J.MATPR.2022.05.453.

[56] J. Aarts, B. van Ravensteijn, H. Fischer, O. Adan, H. Huinink, Polymeric stabilization of salt hydrates for thermochemical energy storage, Appl. Energy 341 (2023), 121068, https://doi.org/10.1016/J.APENERGY.2023.121068.

[57] National Minerals Information Center. U.S. Geological Survey n.d. https://www.usgs.gov/centers/national-minerals-information-center (accessed September 8, 2022)..

[58] Y.I. Aristov, G. Restuccia, G. Cacciola, V.N. Parmon, A family of new working materials for solid sorption air conditioning systems, Appl. Therm. Eng. 22 (2002) 191–204, https://doi.org/10.1016/S1359-4311(01)00072-2.

[59] B.K. Purohit, V.S. Sistla, Inorganic salt hydrate for thermal energy storage application: a review, Energy Storage 3 (2021) e212, https://doi.org/10.1002/EST2.212.

[60] Li J, Zeng T, Kobayashi N, Wu R, Xu H, Deng L, et al. Carbonation Reaction of Lithium Hydroxide during Low Temperature Thermal Energy Storage Process n.d. https://doi.org/10.32604/jrm.2021.015231..

[61] Geological Survey U. Mineral Commodity Summaries 2022 n.d..

[62] M. Kenisarin, K. Mahkamov, Salt hydrates as latent heat storage materials: Thermophysical properties and costs, Sol. Energy Mater. Sol. Cells 145 (2016) 255–286, https://doi.org/10.1016/J.SOLMAT.2015.10.029.

[63] S. Afflerbach, T. Kowald, R. Trettin, Phase transformations during de- and rehydration of scholzite CaZn2(PO4)2·2H2O, J. Solid State Chem. 254 (2017) 184–194, https://doi.org/10.1016/j.jssc.2017.07.028.

[64] A. Jabbari-Hichri, S. Bennici, A. Auroux, Effect of aluminum sulfate addition on the thermal storage performance of mesoporous SBA-15 and MCM-41 materials, Sol. Energy Mater. Sol. Cells 149 (2016) 232–241, https://doi.org/10.1016/J.SOLMAT.2016.01.033.

[65] G.H. Bai, P. Xu, P.C. Li, T.S. Wang, Thermal dehydration kinetic mechanism of aluminum sulfate hydrates, Adv. Mater. Res. 177 (2011) 238–244, https://doi.org/10.4028/WWW.SCIENTIFIC.NET/AMR.177.238.

[66] G. Aylward, T. Findlay, SI Chemical Data Book, sixth ed., John Wiley & Sons Australia, 2008.

[67] N.S. Kotsarenko, V.P. Shmachkova, Catalytic properties of the thermal decomposition products of Zr(SO4)2 · 4H2O, 2002 432, Kinet. Catal. 43 (2002) 280–283, https://doi.org/10.1023/A:1015337031791.

[68] L.J. Struble, P.W. Brown, Evaluation of Ettringite and Related Compounds for Use in Solar Energy Storage. Progress Report, National Engineering Lab.(NBS), Washington, DC (USA), 1984.

[69] H.U. Rammelberg, M. Myrau, T. Schmidt, W.K. Ruck, An Optimization of Salt Hydrates for Thermochemical Heat Storage. Touka Shobo Innov Mater Process Energy Syst Bidyut Baran Saha, Michihisa Koyama, Yasuyuki Tak Yoshinori Hamamoto, Tak Miyazaki, Kohno Masamichi, Kohei Ito IMPRES, 2013, 550–5.

[70] K. Waizumi, H. Masuda, H. Ohtaki, X-ray structural studies of FeBr2·4H2O, CoBr2·4H2O, NiCl2·4H2O and CuBr2·4H2O. cis/trans selectivity in transition metal(II) dihalide tetrahydrate, Inorg. Chim. Acta. 192 (1992) 173–181, https://doi.org/10.1016/S0020-1693(00)80756-2.

[71] R.C. Wheeler, G.B. Frost, A comparative study of the dehydration kinetics of several hydrated salts, Can. J. Chem. 33 (1955) 546–561, https://doi.org/10.1139/v55-064.

[72] A. Gutierrez, S. Ushak, V. Mamani, P. Vargas, C. Barreneche, L.F. Cabeza, et al., Characterization of wastes based on inorganic double salt hydrates as potential thermal energy storage materials, Sol. Energy Mater. Sol. Cells 170 (2017) 149–159, https://doi.org/10.1016/j.solmat.2017.05.036.

[73] A. Makara, Z. Wzorek, M. Banach, Pirofosforany Sodu–Właściwości Fizykochemiczne, Zastosowanie I Metody Produkcji Sodium Pyrophosphates–Physical And Chemical Properties, Applications, 2009.

[74] C.J.J. van Loon, D. Visser, IUCr, Chlorides with the Chrysoberyl Structure: Na2CoCl4 and Na2ZnCl4, vol. 33, 1977, pp. 188–190, https://doi.org/10.1107/S056774087700301X. Urn:Issn:0567-7408.

[75] O.T. Quimby, The chemistry of sodium phosphates, Chem. Rev. 40 (1947).

[76] V.M. Galogaža, E.A. Prodan, V.A. Sotnikova-Yuzhik, D.U. Skala, N.V. Bulavkina, S.I. Pytlev, Some features of thermal behavior of Na5P3O10 · 6H2O, Thermochim. Acta 106 (1986) 141–154, https://doi.org/10.1016/0040-6031(86)85125-5.

[77] E.F. Westrum, Y. Takahashi, N.D. Stout, The heat capacity and thermodynamic properties of hypostoichiometric thorium dicarbide from 5 to 350°K, J. Phys. Chem. 69 (1965) 1520–1524, https://doi.org/10.1021/j100889a014.

[78] A.A.C. Bode, P.G.M. Pulles, M. Lutz, W.J.M. Poulisse, S. Jiang, J.A.M. Meijer, et al., Sodium chloride dihydrate crystals: morphology, nucleation, growth, and inhibition, Cryst. Growth Des. 15 (2015) 3166–3174, https://doi.org/10.1021/ACS.CGD.5B00061/SUPPL_FILE/CG5B00061_SI_002.CIF.

[79] Porter RS, Johnson JF, editors. Analytical Calorimetry. vol. vol. 2. n.d.

[80] T. Yamaguchi, J. Shun-Ichi Hayashi, H. Ohtaki+, X-Ray diffraction and Raman studies of zinc(II) chloride hydrate melts, ZnCl2*/?H20 (R = 1.8, 2.5, 3.0, 4.0, and 6.2), J. Phys. Chem. 93 (1989) 2620–2625.

[81] R.W.M. D'Eye, J.P. Burden, E.A. Harper, The hydrates of zirconium tetrafluoride, J. Inorg. Nucl. Chem. 2 (1956) 192–195, https://doi.org/10.1016/0022-1902(56)80066-3.

[82] B. Chen, F. Kuznik, M. Horgnies, K. Johannes, V. Morin, E. Gengembre, Physicochemical properties of ettringite/meta-ettringite for thermal energy storage: review, Sol. Energy Mater. Sol. Cells 193 (2019) 320–334, https://doi.org/10.1016/J.SOLMAT.2018.12.013.

[83] H.F.W. Taylor, Hydrated calcium silicates. Part V. The water content of calcium silicate hydrate (I), J. Chem. Soc. (1953) 163–171, https://doi.org/10.1039/jr9530000163.

[84] F. Bertsch, B. Mette, S. Asenbeck, H. Kerskes, H. Müller-Steinhagen, Low Temperature Chemical Heat Storage–An Investigation of Hydration Reactions, Proceeding Effstock, New Jersey, 2009.

[85] J. Majzlan, E. Dachs, A. Benisek, J. Plá Sil, J. Sejkora, Thermodynamics, crystal chemistry and structural complexity of the Fe(SO 4) (OH)(H 2 O) x phases: Fe(SO 4)(Thermodynamic properties of uranyl minerals View project Thermodynamics, crystal chemistry and structural complexity of the Fe(SO 4)(OH)(H 2 O) x phases: Fe(SO 4)(OH), metahohmannite, butlerite, parabutlerite, amarantite, hohmannite, and fibroferrite, Artic Eur. J. Miner. (2018), https://doi.org/10.1127/ejm/2017/0029-2677.

[86] F. Marias, P. Neveu, G. Tanguy, P. Papillon, Thermodynamic analysis and experimental study of solid/gas reactor operating in open mode, Energy 66 (2014) 757–765, https://doi.org/10.1016/J.ENERGY.2014.01.101.

[87] R.A. Morgen, R.L. Swoope, The useful life of pyro-, meta-, and tetraphosphates, Cott Ginning Ind. Trust Collect Pap. Work Exptl. Gin. (U S S R) 821 (1931) 57.

[88] A.U. Rehman, M.Z. Shah, A. Ali, T. Zhao, R. Shah, I. Ullah, et al., Thermochemical heat storage ability of ZnSO4·7H2O as potential long-term heat storage material, Int. J. Energy Res. 45 (2021) 4746–4754, https://doi.org/10.1002/ER.6077.

[89] K. Posern, K. Linnow, C. Kaps, M. Steiger, Investigations of ZnSO 4 Hydrates for Solar Heat Storage Applications, vols. 16–9, 2014, https://doi.org/10.18086/eurosun.2014.10.16.

[90] W. Kooijman, D.J. Kok, M.A.R. Blijlevens, H. Meekes, Screening double salt sulfate hydrates for application in thermochemical heat storage, J. Energy Storage 55 (2022) 105459.

[91] X. Zhou, X. Zhang, Q. Zheng, Aluminum ammonium sulfate dodecahydrate with multiple additives as composite phase change materials for thermal energy storage, Energy Fuel. 34 (2020) 7607–7615, https://doi.org/10.1021/ACS.ENERGYFUELS.0C00781/ASSET/IMAGES/LARGE/EF0C00781_0002.JPEG.

[92] C.H. Shomate, Specific heats at low temperatures of (NH4)2SO4, NH4Al(SO4)2 and NH4Al(SO4)2.12H2O, J. Am. Chem. Soc. 67 (1945) 1096–1098, https://doi.org/10.1021/JA01223A022.

[93] J. Stengler, I. Bürger, M. Linder, Thermodynamic and kinetic investigations of the SrBr2 hydration and dehydration reactions for thermochemical energy storage and heat transformation, Appl. Energy 277 (2020), 115432, https://doi.org/10.1016/J.APENERGY.2020.115432.

[94] A. Padamurthy, J. Nandanavanam, P. Rajagopalan, Assessment of selected salt hydrates for thermochemical energy storage applications, Mater. Today Proc. (2022), https://doi.org/10.1016/J.MATPR.2022.04.048.

[95] V.M. Van Essen, J. Cot Gores, L.P.J. Bleijendaal, H.A. Zondag, R. Schuitema, M. Bakker, et al., Characterization of Salt Hydrates for Compact Seasonal Thermochemical Storage, vol. 48906, 2009.

[96] T. Yan, H. Zhang, A critical review of salt hydrates as thermochemical sorption heat storage materials: thermophysical properties and reaction kinetics, Sol. Energy 242 (2022) 157–183, https://doi.org/10.1016/J.SOLENER.2022.07.002.

[97] T.R.S. Gbenou, K. Wang, Kinetic analysis of poly-aluminum sulfate hydrate for low-temperature thermochemical heat storage, Appl. Therm. Eng. 210 (2022), 118317, https://doi.org/10.1016/J.APPLTHERMALENG.2022.118317.

[98] L. Okhrimenko, L. Favergeon, K. Johannes, F. Kuznik, M. Pijolat, Thermodynamic study of MgSO4 – H2O system dehydration at low pressure in view of heat storage, Thermochim. Acta 656 (2017) 135–143, https://doi.org/10.1016/J.TCA.2017.08.015.

[99] K. Posern, C. Kaps, Influences of salt hydrate mixtures and pore sizes on the sorption heat of composite TES materials, in: Proc 11th Int Conf Therm Energy Storage (Effstock 2009), 2009, pp. 1–6.
[100] D. Version, T.H. Storage, An Optimization Of Salt Hydrates For Thermochemical Heat Storage Paper No . Impres2013-117 An Optimization Of Salt Hydrates For Thermochemical Heat Storage, 2014.
[101] H. Jarimi, A. Devrim, Y. Zhang, Y. Ding, O. Ramadan, X. Chen, et al., Materials characterization of innovative composite materials for solar-driven thermochemical heat storage (THS) suitable for building application, Int. J. Low Carbon Technol. 14 (2019) 313–325, https://doi.org/10.1093/IJLCT/CTX017.
[102] Y. Zhang, Q. Miao, X. Jia, Y. Jin, Z. Li, L. Tan, et al., Diatomite-based magnesium sulfate composites for thermochemical energy storage: preparation and performance investigation, Sol. Energy 224 (2021) 907–915, https://doi.org/10.1016/J.SOLENER.2021.05.054.
[103] A. Ur Rehman, M. Khan, Z. Maosheng, Hydration behavior of MgSO 4 -ZnSO 4 composites for long-term thermochemical heat storage application Hydration behavior of MgSO 4 – ZnSO 4 composites for long-term thermochemical heat storage application, J. Energy Storage 26 (2019), 101026, https://doi.org/10.1016/j.est.2019.101026.
[104] M. Zheng, J.W. Luo, Y.H. Zhang, Y.P. Long, Preparation and characterization of composite of MgSO 4 · 7H 2 O and KAl (SO 4) 2 · 12H 2 O thermal storage, Material. In 6th International Conference on Mechatronics, Materials, Biotechnology and Environment (ICMMBE 2016) (2016), p. 280–285.
[105] S. Wei, W. Zhou, R. Han, J. Gao, G. Zhao, Y. Qin, et al., Influence of minerals with different porous structures on thermochemical heat storage performance of CaCl2-based composite sorbents, Sol. Energy Mater. Sol. Cells 243 (2022), 111769, https://doi.org/10.1016/J.SOLMAT.2022.111769.
[106] M. Gaeini, A.L. Rouws, J.W.O. Salari, H.A. Zondag, C.C.M. Rindt, Characterization of microencapsulated and impregnated porous host materials based on calcium chloride for thermochemical energy storage, Appl. Energy 212 (2018) 1165–1177, https://doi.org/10.1016/J.APENERGY.2017.12.131.
[107] P.A.J. Donkers, L. Pel, O.C.G. Adan, Experimental studies for the cyclability of salt hydrates for thermochemical heat storage, J. Energy Storage 5 (2016) 25–32, https://doi.org/10.1016/j.est.2015.11.005.
[108] W. Ji, H. Zhang, S. Liu, Z. Wang, S. Deng, An experimental study on the binary hydrated salt composite zeolite for improving thermochemical energy storage performance, Renew. Energy 194 (2022) 1163–1173, https://doi.org/10.1016/J.RENENE.2022.06.024.
[109] L. Okhrimenko, J. Dussouillez, K. Johannes, F. Kuznik, Thermodynamic equilibrium and kinetic study of lanthanum chloride heptahydrate dehydration for thermal energy storage, J. Energy Storage 48 (2022), 103562, https://doi.org/10.1016/J.EST.2021.103562.
[110] P.E. Marín, Y. Milian, S. Ushak, L.F. Cabeza, M. Grágeda, G.S.F. Shire, Lithium compounds for thermochemical energy storage: a state-of-the-art review and future trends, Renew. Sustain. Energy Rev. 149 (2021), 111381, https://doi.org/10.1016/J.RSER.2021.111381.
[111] W. Li, J.J. Klemeš, Q. Wang, M. Zeng, Characterisation and sorption behaviour of LiOH-LiCl@EG composite sorbents for thermochemical energy storage with controllable thermal upgradeability, Chem. Eng. J. 421 (2021), 129586, https://doi.org/10.1016/J.CEJ.2021.129586.
[112] J. Houben, L. Sögütoglu, P. Donkers, H. Huinink, O. Adan, K2CO3 in closed heat storage systems, Renew. Energy 166 (2020) 35–44, https://doi.org/10.1016/J.RENENE.2020.11.119.
[113] M. Beving, J. Romme, P. Donkers, A. Frijns, C. Rindt, D. Smeulders, Experimental and numerical validation of the one-process modeling approach for the hydration of K2CO3 particles, Process 10 (2022) 547, https://doi.org/10.3390/PR10030547, 2022;10:547.
[114] M. Gaeini, S.A. Shaik, C.C.M. Rindt, Characterization of potassium carbonate salt hydrate for thermochemical energy storage in buildings, Energy Build. 196 (2019) 178–193, https://doi.org/10.1016/j.enbuild.2019.05.029.
[115] K. Kant, A. Shukla, D.M.J. Smeulders, C.C.M. Rindt, Performance analysis of a K2CO3-based thermochemical energy storage system using a honeycomb structured heat exchanger, J. Energy Storage 38 (2021), 102563, https://doi.org/10.1016/J.EST.2021.102563.
[116] Q. Zhao, J. Lin, H. Huang, Z. Xie, Y. Xiao, Enhancement of heat and mass transfer of potassium carbonate-based thermochemical materials for thermal energy storage, J. Energy Storage 50 (2022), 104259, https://doi.org/10.1016/J.EST.2022.104259.
[117] R. Fisher, Y. Ding, A. Sciacovelli, Hydration kinetics of K2CO3, MgCl2 and vermiculite-based composites in view of low-temperature thermochemical energy storage, J. Energy Storage 38 (2021), 102561, https://doi.org/10.1016/J.EST.2021.102561.
[118] A. Chate, R. Sharma, S.M. S, P. Dutta, Studies on a potassium carbonate salt hydrate based thermochemical energy storage system, Energy 258 (2022), 124873, https://doi.org/10.1016/J.ENERGY.2022.124873.
[119] A. Fopah-Lele, J.G. Tamba, A review on the use of SrBr2·6H2O as a potential material for low temperature energy storage systems and building applications, Sol. Energy Mater. Sol. Cells 164 (2017) 175–187, https://doi.org/10.1016/j.solmat.2017.02.018.
[120] B. Michel, N. Mazet, P. Neveu, Experimental investigation of an innovative thermochemical process operating with a hydrate salt and moist air for thermal storage of solar energy: global performance, Appl. Energy 129 (2014) 177–186, https://doi.org/10.1016/j.apenergy.2014.04.073.
[121] N. Mazur, S. Salviati, H. Huinink, A. Fina, F. Carosio, H. Fischer, et al., Impact of polymeric stabilisers on the reaction kinetics of SrBr2, Sol. Energy Mater. Sol. Cells 238 (2022), 111648, https://doi.org/10.1016/j.solmat.2022.111648.
[122] B. Ding, C. Xu, Z. Liao, F. Ye, Study on long-term thermochemical thermal storage performance based on SrBr2-expanded vermiculite composite materials, J. Energy Storage 42 (2021), 103081, https://doi.org/10.1016/J.EST.2021.103081.
[123] W. Li, H. Guo, M. Zeng, Q. Wang, Performance of SrBr2·6H2O based seasonal thermochemical heat storage in a novel multilayered sieve reactor, Energy Convers. Manag. 198 (2019), 111843.
[124] K. Posern, A. Osburg, Determination of the heat storage performance of thermochemical heat storage materials based on SrCl2 and MgSO4, J. Therm. Anal. Calorim. 131 (2018) 2769–2773, https://doi.org/10.1007/S10973-017-6861-8.
[125] R.J. Clark, M. Farid, Experimental investigation into the performance of novel SrCl2-based composite material for thermochemical energy storage, J. Energy Storage 36 (2021), 102390, https://doi.org/10.1016/J.EST.2021.102390.
[126] A. Mehrabadi, M. Farid, New salt hydrate composite for low-grade thermal energy storage, Energy 164 (2018) 194–203, https://doi.org/10.1016/J.ENERGY.2018.08.192.
[127] Y.J. Zhao, R.Z. Wang, T.X. Li, Y. Nomura, Investigation of a 10 kWh sorption heat storage device for effective utilization of low-grade thermal energy, Energy 113 (2016) 739–747, https://doi.org/10.1016/J.ENERGY.2016.07.100.
[128] V. Brancato, L.G. Gordeeva, A.D. Grekova, A. Sapienza, S. Vasta, A. Frazzica, et al., Water adsorption equilibrium and dynamics of LICL/MWCNT/PVA composite for adsorptive heat storage, Sol. Energy Mater. Sol. Cells 193 (2019) 133–140, https://doi.org/10.1016/J.SOLMAT.2019.01.001.
[129] V. Brancato, L.G. Gordeeva, A. Sapienza, V. Palomba, S. Vasta, A.D. Grekova, et al., Experimental characterization of the LiCl/vermiculite composite for sorption heat storage applications, Int. J. Refrig. 105 (2019) 92–100, https://doi.org/10.1016/J.IJREFRIG.2018.08.006.
[130] A.D. Grekova, L.G. Gordeeva, Y.I. Aristov, Composite “LiCl/vermiculite” as advanced water sorbent for thermal energy storage, Appl. Therm. Eng. 124 (2017) 1401–1408, https://doi.org/10.1016/J.APPLTHERMALENG.2017.06.122.
[131] Q. Touloumet, G. Postole, L. Silvester, L. Bois, A. Auroux, Hierarchical aluminum fumarate metal-organic framework - alumina host matrix: design and application to CaCl2 composites for thermochemical heat storage, J. Energy Storage 50 (2022), 104702, https://doi.org/10.1016/J.EST.2022.104702.
[132] N. Gao, L. Deng, J. Li, H. Huang, B. Zhou, Y. Zhou, Multi-form heat storage performance of expanded graphite based CaCl2 composites for low-grade heat source, Energy Rep. 8 (2022) 12117–12125, https://doi.org/10.1016/J.EGYR.2022.09.051.
[133] A. Shkatulov, R. Joosten, H. Fischer, H. Huinink, Core-shell encapsulation of salt hydrates into mesoporous silica shells for thermochemical energy storage, ACS Appl. Energy Mater. 3 (2020) 6860–6869, https://doi.org/10.1021/ACSAEM.0C00971/ASSET/IMAGES/LARGE/AE0C00971_0002.JPEG.
[134] D. Aydin, S.P. Casey, X. Chen, S. Riffat, Numerical and experimental analysis of a novel heat pump driven sorption storage heater, Appl. Energy 211 (2018) 954–974, https://doi.org/10.1016/J.APENERGY.2017.11.102.
[135] T. Nonnen, S. Beckert, K. Gleichmann, A. Brandt, B. Unger, H. Kerskes, et al., A thermochemical long-term heat storage system based on a salt/zeolite composite, Chem. Eng. Technol. 39 (2016) 2427–2434, https://doi.org/10.1002/CEAT.201600301.
[136] Mazur N, Huinink H, Fischer H, Adan O. Under Review: A Systematic Deliquescent Additive Selection Approach for Enhancement of Reaction Kinetics of Thermochemical Heat Storage Materials. - under Review N.d..
[137] N. Mazur, H. Huinink, H. Fischer, P. Donkers, O. Adan, Accelerating the reaction kinetics of K2CO3 through the addition of CsF in the view of thermochemical heat storage, Sol. Energy 242 (2022) 256–266, https://doi.org/10.1016/j.solener.2022.07.023.
[138] J. Houben, A. Shkatulov, H. Huinink, H. Fischer, O. Adan, Caesium doping accelerates the hydration rate of potassium carbonate in thermal energy storage, Sol. Energy Mater. Sol. Cells 251 (2023), 112116, https://doi.org/10.1016/j.solmat.2022.112116.
[139] J.V. Veselovskaya, V.S. Derevschikov, T.Y. Kardash, O.A. Stonkus, T. A. Trubitsina, A.G. Okunev, Direct CO2 capture from ambient air using K2CO3/Al2O3 composite sorbent, Int. J. Greenh. Gas Control 17 (2013) 332–340, https://doi.org/10.1016/j.ijggc.2013.05.006.
[140] L.C. Sögütoglu, M. Steiger, J. Houben, D. Biemans, H.R. Fischer, P. Donkers, et al., Understanding the hydration process of salts: the impact of a nucleation barrier, Cryst. Growth Des. 19 (2019) 2279–2288, https://doi.org/10.1021/acs.cgd.8b01908.
[141] S. Salviati, F. Carosio, G. Saracco, A. Fina, Hydrated salt/graphite/polyelectrolyte organic-inorganic hybrids for efficient thermochemical storage, Nanomaterials 9 (2019), 15121, https://doi.org/10.3390/nano9030420.
[142] S. Salviati, F. Carosio, F. Cantamessa, L. Medina, L.A. Berglund, G. Saracco, et al., Ice-templated nanocellulose porous structure enhances thermochemical storage kinetics in hydrated salt/graphite composites, Renew. Energy 160 (2020) 698–706, https://doi.org/10.1016/j.renene.2020.07.036.
[143] K. Kuwata, S. Masuda, N. Kobayashi, T. Fuse, T. Okamura, K. Kuwata, et al., Thermochemical heat storage performance in the gas/liquid-solid reactions of SrCl2 with NH3, Nat. Resour. 7 (2016) 655–665, https://doi.org/10.4236/NR.2016.711052.
[144] S. Wu, T.X. Li, T. Yan, R.Z. Wang, Experimental investigation on a thermochemical sorption refrigeration prototype using EG/SrCl2–NH3 working pair, Int. J. Refrig. 88 (2018) 8–15, https://doi.org/10.1016/J.IJREFRIG.2017.11.030.

[145] H. Zhang, T. Yan, N. Yu, Z.H. Li, Q.W. Pan, Sorption based long-term thermal energy storage with strontium chloride/ammonia, Energy 239 (2022), 122308, https://doi.org/10.1016/J.ENERGY.2021.122308.
[146] M. Steiger, Thermodynamic properties of SrCl2(aq) from 252 K to 524 K and phase equilibria in the SrCl2–H2O system: implications for thermochemical heat storage, J. Chem. Thermodyn. 120 (2018) 106–115, https://doi.org/10.1016/j.jct.2018.01.017.
[147] N. Yu, R.Z. Wang, Z.S. Lu, L.W. Wang, Development and characterization of silica gel–LiCl composite sorbents for thermal energy storage, Chem. Eng. Sci. 111 (2014) 73–84, https://doi.org/10.1016/J.CES.2014.02.012.
[148] Trading Economics, Lithium Price Chart. MetalaryCom, 2022. https://tradingeconomics.com/commodity/lithium. (Accessed 13 July 2022).
[149] C. Knoll, D. Müller, W. Artner, J.M. Welch, A. Werner, M. Harasek, et al., Probing cycle stability and reversibility in thermochemical energy storage – CaC2O4·H2O as perfect match? Appl. Energy (2017) https://doi.org/10.1016/j.apenergy.2016.11.053.
[150] M. Niermann, Thermodynamische Eigenschaften und Umsatzverhalten von Salzhydraten zur Speicherung und Transformation von Wärme, Staats-und Universitätsbibliothek Hamburg Carl von Ossietzky, 2020.
[151] G. Fang, W. Zhang, M. Yu, K. Meng, X. Tan, Experimental investigation of high performance composite phase change materials based on sodium acetate trihydrate for solar thermal energy storage, Sol. Energy Mater. Sol. Cells 234 (2022), 111418, https://doi.org/10.1016/J.SOLMAT.2021.111418.
[152] T. Xu, S.N. Gunasekara, J.N. Chiu, B. Palm, S. Sawalha, Thermal behavior of a sodium acetate trihydrate-based PCM: T-history and full-scale tests, Appl. Energy 261 (2020), 114432, https://doi.org/10.1016/J.APENERGY.2019.114432.
[153] L.F. Cabeza, G. Svensson, S. Hiebler, H. Mehling, Thermal performance of sodium acetate trihydrate thickened with different materials as phase change energy storage material, Appl. Therm. Eng. 23 (2003) 1697–1704, https://doi.org/10.1016/S1359-4311(03)00107-8.
[154] G. Englmair, C. Moser, S. Furbo, M. Dannemand, J. Fan, Design and functionality of a segmented heat-storage prototype utilizing stable supercooling of sodium acetate trihydrate in a solar heating system, Appl. Energy 221 (2018) 522–534, https://doi.org/10.1016/J.APENERGY.2018.03.124.
[155] H. Ait Ousaleh, S. Sair, A. Zaki, A. Younes, A. Faik, A. El Bouari, Advanced experimental investigation of double hydrated salts and their composite for improved cycling stability and metal compatibility for long-term heat storage technologies, Renew. Energy 162 (2020) 447–457, https://doi.org/10.1016/J.RENENE.2020.08.085.
[156] H. Ait Ousaleh, S. Sair, A. Zaki, A. Faik, J. Mirena Igartua, A. El Bouari, Double hydrates salt as sustainable thermochemical energy storage materials: evaluation of dehydration behavior and structural phase transition reversibility, Sol. Energy 201 (2020) 846–856, https://doi.org/10.1016/J.SOLENER.2020.03.067.
[157] Евгений Геннадиевич Афонин ЕГА, RU2307793C2 - Method of Production of the Zinc-Ammonium Sulfate Hexahydrate - Google Patents, 2005.
[158] G.A. Lane, Solar Heat Storage: Volume II: Latent Heat Material, CRC Press Inc., 2018.
[159] A. Niwa, N. Kobayashi, Calcium bromide hydration for heat storage systems, Cogent Eng. 2 (2015), https://doi.org/10.1080/23311916.2015.1064218.
[160] T. Kito, Y. Osaka, K. Kuwata, N. Kobayashi, H. Huang, Z. He, Study on performance of chemical heat storage system for direct steam generation, J. Renew. Sustain. Energy 6 (2014), 23101, https://doi.org/10.1063/1.4868029/285425.
[161] J. Galovic, P. Hofmann, Thermochemical heat storage for consumption reduction in internal combustion engines, MTZ Worldw 80 (2019 807 2019) 134–139, https://doi.org/10.1007/S38313-019-0085-1.
[162] D. Liu, L. Xin-Feng, L. Bo, Z. Si-quan, X. Yan, Progress in thermochemical energy storage for concentrated solar power: a review, Int. J. Energy Res. 42 (2018) 4546–4561, https://doi.org/10.1002/ER.4183.
[163] D. Chen, X. Chen, Z. Ma, Y. Wang, A.P. Roskilly, J. Zhou, et al., Experimental study of LiCl/LiBr-zeolite composite adsorbent for thermochemical heat storage, Build 12 (2022) 2001, https://doi.org/10.3390/BUILDINGS12112001, 2022;12:2001.
[164] T. Roger, S. Gbenou, A. Fopah-Lele, K. Wang, J. Krzywanski, K. Grabowska, Recent status and prospects on thermochemical heat storage processes and applications, Entropy 23 (2021) 953, https://doi.org/10.3390/E23080953, 2021;23:953.
[165] Y. Yin, Z. Yuan, X. Li, Rechargeable aqueous zinc–bromine batteries: an overview and future perspectives, Phys. Chem. Chem. Phys. 23 (2021) 26070–26084, https://doi.org/10.1039/D1CP03987C.